MICROWAVE INTERFERENCE DUE TO RAIN SCATTER AT Ku AND Ka - BANDS IN AKURE, SOUTH WEST, NIGERIA

ALAO, OLUMUYIWA ADEMOLA
(PHY/96/8269)

A THESIS SUBMITTED IN PARTIAL FULFILLMENT OF THE REQUIREMENT FOR THE AWARD OF THE DEGREE

OF

MASTER OF TECHNOLOGY (M. TECH)

IN

COMMUNICATION PHYSICS

DEPARTMENT OF PHYSICS

FEDERAL UNIVERSITY OF TECHNOLOGY AKURE, ONDO STATE, NIGERIA

DECEMBER, 2010

CERTIFICATION

Certification by the Student

This work has not been presented elsewhere for the award of a degree, or any other purpose.

Candidate's Name: ALAO, Olumuyiwa Ademola

Signature..... Date.22/12/2010

Certification by the Supervisors

We hereby certify that this research work was carried out by ALAO, Olumuyiwa Ademola, in the Department of Physics, Federal University of Technology, Akure under our joint supervision.

..... 22/12/2010.....

Prof. M.O. Ajewole — Date

(Major Supervisor)

..... 05/01/2011.....

Dr. J.S. Ojo — Date

(Co-Supervisor)

..... 05.01.11.....

Prof. (Mrs) I. A. Fuwape — Date

Head of Department

DEDICATION

This work is dedicated to Almighty God in acknowledgement of His infinite mercy and love for mankind.

ACKNOWLEDGEMENTS

I give my sincere gratitude to the author of all knowledge, wisdom, understanding and the blessed Trinity for the outstanding skills used in carrying out such an interesting research. All glory, laud and honour are to Him the Most High.

My unlimited and sincere appreciation goes to my supervisor Prof. M.O. Ajewole for his guidance and particularly his concerns and fatherly care, all towards the success of this project. I will not forget to mention his useful suggestions, thorough supervision and his assistance in making his library available for me, in order to make this work a success. I quite appreciate him.

I acknowledge with thanks the encouragement received from the members of staff of the Department of Physics, Federal University of Technology, Akure, most especially my co-supervisor Dr. J.S. Ojo for his readiness to attend to every of my complaint everywhere, Dr. M.T. Babalola, Dr. E.O. Ogolo, Dr. A.M. Arogunjo, Dr. O.S. Ajayi, Dr. A.B. Rabiu, Dr. S.S Oluyamo, Dr O.R. Oladosu, Dr. A.T. Adediji, Mr K.D. Adedayo, and Mr O.I. Olusola for their readiness to assist in the course of this research.

I cannot fail to express my special thanks to my H.O.D, Prof (Mrs) I.A. Fuwape, for her words of encouragement, assistance and succour in times of need.

A very profound appreciation goes to my loving parents, Mr. and Mrs. G.A Alao, also to my brothers and sisters, Mr. Adeyemi Alao, Master Oluseye Alao, Mrs Bimbola Wahab and Miss Oluwaseun Alao for their moral contributions, words of encouragement and financial support towards the success of this work.

I am also indebted to my divine father, Rev. M.O. Onayemi for his unceasing prayer for me towards my academic success. I acknowledge my siblings, for their assistance throughout the season of this research work.

TABLE OF CONTENTS

CHAPTER THREE

CHAPTER FOUR

CHAPTER FIVE

LIST OF FIGURES

LIST OF TABLES

ABSTRACT

The strong impact of rain on satellite-based telecommunication systems makes the prediction of rain induced propagation impairments (such as attenuation and interference) using the cumulative distribution of the point rainfall intensity a subject of continuous research interest. Tropical rainfall has interesting characteristics, which are quite distinct from those of temperate rainfall; and therefore have dire consequences on the quality of signal at Super High Frequencies (SHF). For the prediction of interference, many models and techniques have been used for determining interference due to hydrometeor (raindrop) scatter between independent microwave stations. The present study employs the modified version of the three dimensional (3D) rain cell model to estimate microwave interference due to rain scattering. It uses as input three elevation angles, 55^0 (over the Atlantic Ocean Region), 23^0 (over Indian Ocean Region) and 42.5^0 (NIGCOMSAT -1 geostationary satellite) in the analysis of transmission loss. The transmission loss and effective transmission loss statistics are computed at frequencies ranging between 4 – 35 GHz used for satellite and terrestrial communication. However, in computing the transmission loss and the effective transmission loss, both horizontally and vertically polarized radio signals are assumed to pass through the rain medium. Results are presented for thunderstorm rainfall type which is prevalent in the tropical region. Results are also presented for the variation of transmission loss particularly for the Ku (11/14 GHz) and Ka (20/30 GHz) frequency bands. Also, the estimation of the statistics of the transmission loss are computed for varying distances from the terrestrial system (TS) antenna to the common volume (CV) formed by the intersection of the antenna beams for all the look angles. The study also considered the transmission loss effects at two path length configurations; short ($\leq$ 50km) and long (> 50km) , varying antenna gains and varying percentage time unavailabilities (outage time) for vertical and horizontal polarizations. The results obtained were then used to predict the severity of rain scattering resulting in intersystem interference, particularly at frequencies ranging from 4 – 35 GHz currently in use by most communication satellite systems.

CHAPTER ONE

1.0 INTRODUCTION

Rain induced propagation impairments such as attenuation and interference cause various degrading effects to the propagation of millimeter wave signals. The signal propagating through the clear air suffers reflection and refraction due to inhomogeneity in the atmospheric radio refractive index. In precipitation medium, a radio signal suffers attenuation, phase rotation and depolarization (Holt et al., 1992). This phenomenon results into scattering known as *bistatic scattering* which gives rise to intersystem and inter-service interference. Hence, the increase in usage of existing shared frequency band between satellite and other services, call for accurate technique for predicting radio interference level. Propagation effects play a fundamental role in virtually all interference geometries. However, at super high frequencies [SHF] and extra high frequencies [EHF], scatter by liquid and frozen water particulates (Hydrometeor) in the atmosphere can become the dominant interference mechanism (Olsen, 1993). Duct propagation is usually the dominant interference mechanism over a terrestrial path between a fixed –service transmitter and the earth station antenna pointing in its general direction. However hydrometeor scatter is often the dominant mechanism for an earth station antenna pointed in the opposite direction. Hence, on interference path between space and earth and vice versa, hydrometeor scatter effects are almost always dominant (Olsen,1993).

Interference has been the subject of international concern due to its nature. The international advisory body on radio matters for the International Telecommunication Union [ITU], the International Radio Consultative Committee [CCIR] [as of April, 1993 recognized as the Radio communicator sector] has prime responsibility in establishing the technical bases for such regulation (Olsen, 1993). Integrated Service Digital Networks [ISDN] connection via satellite for telephony and data communication, internet services relying on very small aperture terminals [VSATs] system satellite television, remote sensing of environment among others are typical services which depend on satellite communication for reliable and efficient service delivery.

The bistatic hydrometeor interference is due to intersection of a terrestrial beam and an earth station beam, the interference will result in the decrease of the signal to noise ratio at the interfered terminal and thus lead to link outage depending on the severity of the received interference levels. Viewing the extent of such interference on statistical terms is significant for service planner and designers so as to be able to assess the degree of energy coupling between the systems (Ajewole et al.,1999).

For the prediction of interference, the following parameters are needed to calculate the transmission loss due to hydrometeor scatter between two microwave stations. These parameters are the electrical system and meteorological variables. A lot of models backed with experimental validations have been proposed and tested using data from temperate region. However, in the tropical region including tropical Africa, the problem of interference due to rain scattering began to receive attention in the last 10 years. Modest contributions have been made in Africa, by the work of Ajewole et al., 1999, Ajewole, 2003, Ajewole and Ojo, 2005, Ojo et al., 2008, Ojo and Ajewole, 2010. Several models have been proposed for the prediction of interference due to hydrometeors, among these models, the ones based on the assumption of an exponential rain cell model are Capsoni et al., 1987a and Capsoni and D'Amico,1997 and Awaka, 1989.

1.1 OBJECTIVES OF THE STUDY

The specific objectives of this research are to:

(a) compute the transmission loss and effective transmission loss for vertically and horizontally polarized signals; and

(b) predict the occurrence of satellite signal outage during transmission through heavy tropical rainfall.

1.2 EXPECTED CONTRIBUTIONS OF THE RESEARCH TO KNOWLEDGE

The findings of the research are to establish:

(a) criteria for planning acceptable satellite communication network that will reduce interference from terrestrial broadcasts; and

(b) statistics of the transmission loss which will assist in the coordination, sharing and utilization of frequencies in order to minimize severe losses due to interference and congestion.

1.3 THE SCOPE OF THE STUDY

In this dissertation, factors such as antenna beamwidth, antenna gain and antenna distance to the common volume formed by the intersecting signals that can affect the availability of wanted signal in a tropical location are investigated. Emphasis is on the availability of satellite channels receiving interfering signals from terrestrial microwave relay link operating at the same frequency due to rain scatter in the common volume formed by the intersection of their antenna beam. The study is limited to the frequency range of 4 -35 GHz and for horizontally and vertically polarized radio signals passing through the rain medium. The study also focuses attention on the possibility of a terrestrial point to point microwave radio interfering with the reception of satellite traffics over both short ($\leq$ 50km) and long (> 50km) path lengths in a tropical location. The terrestrial station antenna gain was varied from 35 -55dB and probability of occurrence ranged from $1\text{-}10^{-4}$% of time. The cumulative distribution of point rainfall rate measured at Akure, (Long $5^0\ 11^1$ E, Lat $7^0\ 15^1$N) was used. The results obtained were used to predict the severity of rain scattering particularly at Ku and Ka bands during heavy rainfall activity.

CHAPTER TWO

LITERATURE REVIEW

2.1 DEFINITIONS OF SOME IMPORTANT TERMS

The two dimensional visualization of rain rate structures define the characteristics of rain rate field or intensity. The method for simulating typical rain rate fields provides an important tool to the designer of communication systems.

a) RAIN RATE

The rain rate is defined as the number of raindrops falling in a particular region per unit time. It is measured in mm/h.

b) RAIN CELL STRUCTURE

The rain cell structure is assumed to have cylindrical symmetry. Within the horizontal cross-section of the cell, the rainfall rate is assumed to be distributed exponentially (Awaka, 1989).

Scattering occurs only within the rain cells having circular cross-section whose diameter depend on the rainfall rates inside the cell. Attenuation also occurs inside as well as outside the rain cell, but only below the rain height inside the cell, the well known dependence of specific attenuation on the rainfall rate is assumed.

$$R(r) = R_M \exp\left(\frac{-r}{\rho_o}\right) \qquad (2.1)$$

Equation (2.1) defines the point of rain intensity for a typical exponential rain structure. Here r is the radial distance from the center of the rain cell, R_M is the peak rain rate at the center and ρ_o is a characteristic distance from the cell center over which the rain intensity reduces to exp (-1) of the peak value.

An example of the horizontal cross section of a rain cell is shown in figure (2.1), where r is the radial distance from the rain cell center , R_m is the maximum rainfall rate and R_{min} is the minimum rainfall rate.

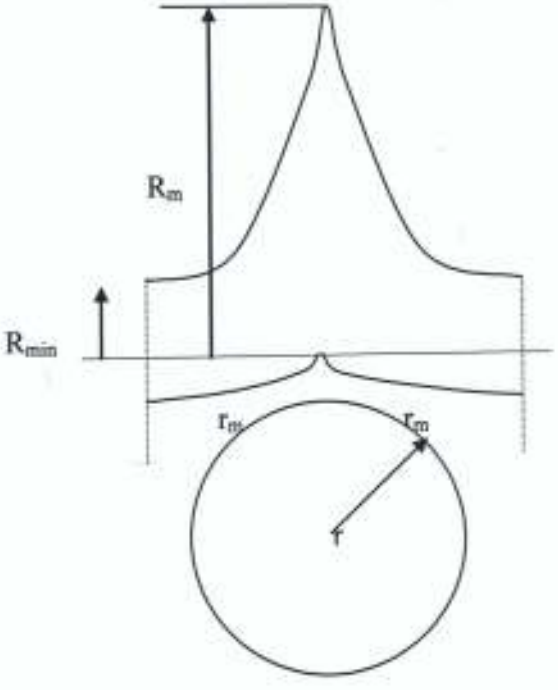

Fig. 2.1 Horizontal cross section of rain cell

2.2 RAIN SCATTERING

Attenuation due to rain plays a significant role in the design of earth- satellite radio links at frequencies above 10 GHz. The increasing demand for the frequencies for telecommunication services has aroused increased interest in the study of radio wave attenuation due to rainfall on earth –satellite radio paths. Most of the attenuation studies on earth –satellite paths have been carried out in the temperate region of the world. The increasing use of satellites for telecommunications in tropical locations such as Nigeria has necessitated more than before the need for earth – space attenuation studies in the tropics.

2.3 INTERFERENCE

The interference caused by hydrometeor scatter is the dominant mechanism for scattering geometries. With the increase usage of existing shared frequency band between satellite and other communication links, accurate techniques for predicting interference levels are necessary. Propagation effects play a fundamental role in virtually all interference geometries. At SHF and EHF, scatter by rain (hydrometeor) in the atmosphere can become the dominant interference mechanism (Olsen, 1993).

Duct propagation is usually the dominant interference mechanism over a terrestrial path between a fixed service transmitter and the earth – station antenna pointing in its general direction, Hydrometeor scatter is often the dominant mechanism for an earth – station antenna pointed in the opposite direction. Interference is however, a subject of international agreement. The radio regulations governed the citing of earth stations that might interfere with terrestrial receiver (and vise versa) across international boundaries. Other radio regulations deal with other interference geometries and services (Olsen,1993).

Many propagation mechanisms can contribute to interference fields, including the line of sight propagation, tropospheric scatter, diffraction by terrain and buildings, refraction and ducting by elevated surface layers. Hydrometeor scatter depends on path geometries, terminal separation, system parameters such as antenna directivity, frequency, tolerance to interference, and local climatic factor. Hence, for all interference geometries, the goal is to minimize permissible separation between terminals within the allowable levels of interference (Olsen,1993).

2.3 INTERFERENCE MODELS

A lot of models and prediction techniques have been used for determining interference due to hydrometeor scatter between two independent microwave stations. Among the most widely used models are; International Radio Consultative Committee (CCIR) Model report 569 (1990) as reported in COST 210, International Telecommunication Union –Bureau of Radio Communication (ITU-R) Model, Capsoni Model, Crane Model, Awaka Model, Gaussian Profile Model, and the simplified 3D cell Model among others. The present study employs the modified 3D cell model of Awaka in the computation (Awaka,1989).

2.4 A SURVEY OF SOME EXISTING INTERFERENCE MODELS

2.4.1. CCIR Model

This is defined as the International Radio Consultative committee CCIR model intended for the prediction of transmission loss statistics from rain fall rate statistics. It is based on two fundamental assumptions;

1. Scattering which occurs only within the rain cells having circular cross section and whose diameter depends on the rainfall rates inside the cells.
2. Attenuation which occurs within and without the rain cell, and only below the rain height.

Observation of existing statistics of measured data above 10 GHz, specifically 11-18 GHz range seems to show reasonable agreement with the predictions on the basis of CCIR model (COST 210, Report 569,1990). At higher frequencies, 30GHz and above, larger deviation have been observed. One other assumption is that the time invariant rain height determines whether the scattering occurs in the rain or in the ice region.

In the CCIR Model, the expression used for determining transmission loss at frequency f, is (Olsen,1993):

$$L = 168 + 20\log r - 20\log f - 13.2\log R - g_r + 10\log A_b - \log C + \tau + \gamma_o d_o + \gamma_w d_w \quad (2.2)$$

where:

r *is* the distance between the maximum scattering point and the location of the earth station antenna.

R is the surface rainfall rate (mm/h) for the required climatic region.

g_T is the terrestrial station antenna.

A_b is a correction factor for non – Rayleigh scattering.

C is the effective scatter transfer and is expressed as

$$C = \frac{2.17}{\gamma_R d_S}\left(1 - 10^{-\gamma_R d_S/5}\right) \qquad f > 4\ \text{GHz} \qquad (2.3)$$

$$= 1 \qquad f \leq 4\ \text{GHz} \qquad (2.4)$$

$\gamma_o d_o + \gamma_w d_w$ are the atmospheric attenuation for Oxygen and water vapour respectively.

$$d_S = 3.5R^{0.08} \qquad \text{km} \qquad (2.5)$$

$$\tau = 631kR^{\alpha-0.5}.10^{-(R+1)^{0.25}} \qquad dB \qquad (2.6)$$

2.4.2. ITU-R Model

This model predicts the distribution of rainfall rate in a region. It investigates the problem of hydrometeor interference by assuming the 3D exponential rain cell model of Capsoni et al., (1997). The model offers possibility of predicting the statistics of many propagation parameters such as attenuation, interference by rain scattering etc, which are determined by rain cell characteristics and their frequency of occurrence. The model has some limitation such as yielding excessively large rain cell radius when rain intensity is less or equal to 6mm/h, and overestimating the attenuation of the wanted signal in the computation of the effective transmission loss. Also, the non-inclusion of the relationship between the reflectivity factor and the attenuation on one hand, and the assumption of the fixed rain cell position in space is another limitation of the model.

2.4.3 LOG - NORMAL MODEL

Log- normal model is a prediction method to the rain scattering problem which produces a successful result in the estimation of interference levels. The applicability of the model assumes the uniformity of precipitation within the scattering volume described by a cell model which is simple in a sense that assumes a fixed cylindrical rain cell. This interference level changes depending on the location of scattering volume relative to the cell. However, the fixed cell does not provide all possible levels of interferences (Ajewole, 2003).

2.4.4 3D CELL MODEL

The three dimensional rain cell model (3D) is deployed to examine a non fixed cell situation and to improve the limitations associated with the models discussed earlier on. Hydrometeor scattering is observed when a rain cell passes through the common volume, which is defined by the intersection of the antenna main lobes (COST 210). At any time, the transmission loss can be computed by the Bistatic Radar Equation (BRE) if the location and structure of the rain cell are specified. The computed transmission loss may vary with time because of the temporal change in the rain cell structure. For simplicity, this work assumes that the rain cell structure does not change with time. Then the temporal changes in transmission loss occur only because of the movement of the rain cell (Awaka,1989). Hydrometeor scattering is observed when a rain cell overlaps with the common volume. After the rain cell moves away from the common volume, no hydrometeor scattering will be observed for a while. Then there comes another rain cell with different size and intensity into the region of the common volume, and hydrometeor scattering will resume. When this process continues for a long while, all possible values of the transmission loss are obtained.

2.4.4.1 RAIN CELL MOVEMENT

Rain cells are assumed to have constant velocity. Considering identical rain cells, though the cells are identical in structure, the closest distance between the centre of the cell and the center of the common volume, which is a similar concept to the impact parameter in the collision theory varies with each cell. This closest distance is assumed distributed uniformly in statistical senses (Awaka, 1989). In actual fact, the center of the common volume is located at a fixed point whereas the rain cells move about. However, since the rain cells are assumed to be identical and are also assumed to have the same

velocity, the actual situation can be regarded as equivalent to the following situation in a statistical sense. A rain cell is fixed in space whereas the center of the common volume moves about uniformly on a horizontal plane in the rain cell. We also assume that each type of rain cell contains infinite number of identical cells crossing the common volume. The values of the transmission loss vary depending on the position of the center of the common volume in the rain cell. The above statistically identical situation enables us to compute the cumulative distribution of transmission loss.

2.4.4.2 SPATIAL STRUCTURE OF RAIN CELL

The spatial structure of precipitation rate (mm/h) in both vertical and horizontal direction is needed to compute statistics of the transmission loss. The vertical structure of precipitation assumes that rainfall rate is vertically homogeneous up to the effective rain height (Ajewole et al.,1999).

The radar reflectivity is a useful parameter for defining the vertical structure of rain. The vertical structure of precipitation is assumed constant up to the 0^0C isotherm height, below which is the rain region where attenuation and scattering of the wanted and the interfering signals occur. Beyond the 0^0C, is the ice region where radar reflectivity, Z decreases at the rate of 6.5 dB/Km (Ajewole, 2003) hence, attenuation is small, Z is climate and region dependent. It varies in the temperate region, while it is relatively stable in the tropical climates. The physical rain height on the other hand is a more practical quantity for defining the height of the rain region especially for rainy conditions (Ajayi and Barbaliscia,1990). The expression proposed by the ITU-R for the mean 0^0C isotherm height h_0 which can be equated to the mean 0^0C isotherm height h_{FR} during raining conditions in the tropical region is

$$h_{FR} = 5.0km \qquad 0 < \phi \leq 23^0 \tag{2.7}$$

ϕ is the latitude of the locations. Due to the model's over-estimation of the h_{FR} worldwide. (Ajayi and Babaliscia, 1990) used radiosonde data to propose a relationship for h_{FR} for Nigeria. This relationship depends weakly on the rain rate value averaged over a 2hr period, 1hr before and 1hr after the launch of the radiosonde. It is expressed as

$$h_{FR} = 4.67 + 6\times10^{-3}R \tag{2.8}$$

2.4.5 THE COMPLETE 3-D BISTATIC RADAR EQUATION (BRE)

Bistatic interference due to hydrometeors within the common volume of two antenna beam is modeled by the bistatic radar equation. The bistatic interference (coupling) between the two independent communication links operating at the same frequency is generally evaluated in terms of the bistatic radar equation (BRE), i.e. the ratio of signal power in the two systems (Crane, 1974). If multiple scattering by atmospheric particles is negligible, BRE is expressed as:

$$\frac{P_r}{P_t} = G_t(i)G_r(0)\frac{\lambda^2}{(4\pi)^3}\int_{cv}\frac{F_t(\partial_1,\phi_1)F_r(\partial_2,\phi_2)A_t(R_1)A_r(R_2)A_g}{R_1^2R_2^2}dV\int_0^\infty N(D)\sigma_s(i,o,D)dD \tag{2.9}$$

where; P_t and P_r are the transmitted interfering power and the receive power at the interfered station.

- $F_{(t/r)}(\partial,\phi)$ represents the directivity function of the antenna systems from which the effective areas are calculated.

$-A_{(t|r)}(R)$ represents the attenuation along the paths from and towards the elementary volume.

A_g is the attenuation due to gaseous absorption. $G_{(t|r)}$ are the transmitter and receiver antenna gains.

$-\lambda$ is the wavelength of the radio signal.

$-R_{(1|2)}$ represents the path length from the transmitter to the common volume and from the common volume to the receiver.

$-$D is the particle equivolumic diameter,

$-N(D)$ is the particle number density in a diameter interval dD

$-\sigma_s$ is the total scattering cross section of particles with diameter D inside the common volume and it is related to the reflectivity factor, point rain rate R, and the complex refractive index of the rain drops.

2.4.5.1 THE SIMPLIFIED BISTATIC RADAR EQUATION

The common volume is assumed to be very small as compared to R_1 and R_2 in equation (2.9). A_t and A_r are assumed independent of their positions in the common volume, and the total scattering cross section is also assumed constant within the common volume. Hence the simplified form of the complete 3 D BRE (Capsoni et al.,1992) is expressed as:

$$\frac{P_r}{P_t} = \frac{A_t(R_1)A_r(R_2)A_g G_t(i)G_r(0)\lambda^2\sigma_{bi}}{(4\pi)^3 R_1^2 R_2^2} \times \int_0^\infty F_t(\partial_1,\phi_1)F_r(\partial_2,\phi_2)dV \qquad (2.10)$$

The symbols are as defined previously in equation (2.9), while the scattering cross section per unit volume of precipitation replaces the second integral term on the far right of equation (2.10). This quantity depends on the frequency and polarization of the incident and scattered signal and on the value of the refractive index, size and shape of the hydrometeor, among others.

For interference simulations and prediction, it is convenient to take into consideration the worst case, since the highest value of coupling occurs when the transmitted and received signals are both vertically polarized whatever the scattering angle (Awaka and Oguchi, 1982). Hence spherical drops are chosen and vertical polarization is assumed. The scattering cross section of each single particle can then be evaluated numerically using the complete Mie solution or Rayleigh approximation. At frequencies less than 10GHz, the scattering cross section per unit volume of precipitation σ_{bi} is expressed as:

$$(10^{18})\frac{\pi^5}{\lambda^4}\sigma_{bi} = \left|\frac{\varepsilon-1}{\varepsilon-2}\right|^2 Z \qquad (2.11)$$

where λ is the wavelength in meters, ε is the permittivity of the medium (that is frequency, temperature and particle phase dependent) and Z (mm^6m^{-3}) is the so called radar reflectivity which is proportional to the sixth power of the drop diameter, that is:

$$Z = \int_0^\infty N(D)D^6 dD = \int_0^\infty N_0 e^{-\Lambda D} D^6 dD \tag{2.12}$$

where $N(D)dD$ is the density of raindrops in a diameter interval dD, N_0 =8000 $(m^3 mm^{-1})$ and Λ =$4.1R^{-0.21}$ (mm^{-1}) (Marshall and Palmer, 1948). The integration in equation (2.12) can be avoided by using a power law relation of the form

$$Z = a\,R^{b} \tag{2.13}$$

R Is the rainfall rate (mm/h). Then,

$$Z = 10\log z \tag{2.14}$$

For tropical thunderstorm rain type assumed in this study, the parameters for ' a ' and ' b' of equation (2.13) are 'a ' =461 and ' b ' = 1.31 respectively (Ajayi and Owolabi, 1987). For vertical polarization the total scattering cross section is the ratio of the analogous quantity in the Rayleigh regime and a correcting factor S, that is,

$$\sigma\left(\hat{i},\hat{o}\right) = \sigma_{Ri}\left(\hat{i},\hat{o}\right)/S \tag{2.15}$$

where σ_{Ri} is defined by equation (2.11) and

$$10\log S = R^{0.4}10^{-3}\left[4(f-10)^{1.6}\left(\frac{1+\cos\phi_s}{2}\right)+5(f-10)^{1.7}\left(\frac{1-\cos\phi_s}{2}\right)\right] \tag{2.16}$$

Note that $10\log S = 0$, if $f \leq 10GHz$ where f *is the* frequency (GHz) and ϕ_s is the scattering angle. Using equation (2.13) multiplied by the constant in equation (2.11) and replacing the second integral on the far right of equation (2.9) by this new quantity, we are then left with the integral on the far right of equation (2.10) defined as the effective common volume, V_m

$$V_m = \int_v \frac{F_1(\partial_1,\phi_{12})F_r(\partial_2,\phi_2)}{R_1^2 R_2^2} dV \tag{2.17}$$

2.4.6 TRANSMISSION LOSS

For a given power radiated by an interfering terminal there will be a threshold power received by the victim terminal above which the interference is unacceptable. The ratio of the received power to (transmitted) power is termed the TRANSMISSION LOSS. Hence interference level can be evaluated in terms of the transmission loss which is the inverse of equation (2.10) using the expression,

$$L = 10\log\left(\frac{P_t}{P_r}\right) \tag{2.18}$$

Equation (2.10) depends on several factors, (geometric, electrical and meteorological)and these are independent, as such, it is very difficult to evaluate together once. Nevertheless, utilizing the pencil beam approximation, in which the common volume is assumed to be very small compared to the distances R_1 and R_2 in the denominator of equation (2.9), A_t and A_r are assumed independent of their position in the common volume, and the total scattering cross section is also assumed constant within the common volume. The above assumption yield the simplified form of the complete 3 D bistatic radar equation which is expressed as:

$$\frac{P_r}{P_t} = \frac{A_t(R_1)A_r(R_2)A_g G_t(i)G_r(0)\lambda^2\sigma_{bi}}{(4\pi)^3 R_1^2 R_2^2} \times \int_0^\infty F_t(\partial_1,\phi_1)F_r(\partial_2,\phi_2)dV \tag{2.19}$$

The ITU recommends that the transmission loss should be used for the evaluation of the level of interference due to hydrometeor scattering. This transmission loss is simplified in the difference of the transmitted power and the received power especially when antenna feeder losses are absent. Thus, equation (2.18) becomes:

$$L = P_t - P_r \qquad \text{(dB)} \tag{2.20}$$

2.4.7 EFFECTIVE TRANSMISSION LOSS

The effective transmission loss is defined as the transmission loss minus the extra attenuation suffered by the wanted signal (Capsoni and D' Amico, 1997). It is usually evaluated on the basis of a joint and conditioned statistics of the transmission loss and the extra attenuation. It is therefore expressed as:

$$L_e = L - A_w = P_t - (P_r + A_w) \qquad \text{(dB)} \tag{2.21}$$

L is the transmission loss defined as the ratio of the interfering transmitted power P_t to the interfering received power P_r at the interfered station, and is evaluated using the Bistatic Radar Equation (BRE). A_w is the extra attenuation on the wanted signal. Using the simplified form of the BRE (Capsoni et al., 1992), the transmission loss L is calculated from equation (2.20)

CHAPTER THREE

3.0 RESEARCH METHODOLOGY

This involves the evaluation procedure of the simplified 3-D bistatic radar equation and the exponential rain cell model. The model computes the cumulative distribution of transmission loss and effective transmission loss at different frequencies in the Ku, Ka and higher bands. These are calculated for the vertical and horizontal polarized radio signals on the tropical paths. The interfering terrestrial system for this study has an elevation angle of 1^0, beamwidth of 1.6^0 and gains varying from 35 -55 dB. The interfered station is a narrow beam width 0.18^0, downlink earth satellite receiver having a gain of 59dB and oriented at an elevation angle of 55^0. This is the look angle of most satellite receiver system over the Atlantic Ocean region in the tropics, while the rest is through the Indian Ocean region at an elevation angle of 23^0. As a partial validation of the described rain rate characteristics on radio signals evaluation technique, the fade distribution was also calculated at 42.5^0 been the look angle of the NIGCOMSAT 1 geostationary satellite. This study also considered the variation for other elevation angles such as 55^0 and23^0.

3.1 THEORETICAL CONSIDERATION

The horizontal structure of rain rate are usually assumed to be exponentially distributed with peak intensity inside the rain cell,(Capsoni et al.,1987b) expressed as:

$$R(r) = R_M \exp\left(\frac{-r}{r_0}\right) \quad , \tag{3.1}$$

where r is the radial distance from the center of the rain cell. R_M is the peak rain rate at the center, and r_0 is the "characteristic distance" from the cell center over which the rain intensity reduced to exp (-1) of the peak value and this corresponds to the minimum rain rate in the cells. For the Awaka model used in this study, r_0 is expressed as:

$$r_0 = \frac{10 - 1.5\log_{10} R_M}{\ln\left(\frac{R_M}{0.4}\right)} \quad \text{(km)} \tag{3.2}$$

The probability of occurrence of a rain cell is defined in terms of the total number of rain cells, $N(R_M)$. $N(R_M)$ for a given area per unit rain rate R(r). A general retrieval algorithm for, $N(R_M)$ as proposed by Awaka can be expressed as :

$$N(R_M) = -\left(\frac{1}{2\pi r_0^2 R_M}\right)\frac{d^3P(R)}{d(\ln R)^3} \quad \Big| \; R = R_M \tag{3.3}$$

By using third order differentiation this equation is solved in terms of a power law relationship for the cumulative distribution of measured rain rate P(R) at the location of interest as:

$$P(R) = P_o\left(\ln\frac{R'}{R}\right)^K \qquad 0 < \; R \; < R' \tag{3.4}$$

P_o and k are easily obtained by interpolation from cumulative distribution of the measured point rain rate $P(R)$. R' (mm/h) is assumed to be about four times the highest rain rate at the location.

3.2 INPUT PARAMETERS NEEDED FOR THE COMPUTATION OF TRANSMISSION LOSS.

A coupling prediction program is the simplified 3D cell Model employed for the computation of the transmission loss and the effective transmission loss for the bistatic polarization. The modeling requires some input parameters, which include the local meteorological information of the tropical location, the geometrical and electrical properties of the link.

Input parameters for the electrical characteristics of the link include; antenna gains, antenna beam widths, operating frequencies and antenna polarization. The geometrical information includes; antenna pointing (azimuth) and distance between the stations with respect to common volume reference system. The meteorological information required includes 0^0 isotherm height, cumulative distribution of modeled point rainfall rate and rain freezing height (h_{FR}). While the 3D algorithm is used, the ITU-R recommended procedure for computing the transmission loss and the effective transmission loss. The basic input parameters used in the evaluations in this study are as follows:

3.2.1 PATH GEOMETRY

This study has the station separation distance between 50.7 km for short path length and 255.4km for long path length.

3.2.2 SYSTEM PARAMETERS

The satellite earth station is defined as the interfered station. Its satellite is assumed to have an angle of 55^0 which is the look angle of most satellite receivers over the Atlantic Ocean region in Nigeria. The interfering terrestrial system for this study has an elevation angle of 1^0 with beam-width of 1.6^0 and antenna gain varying from 35 – 55dB. The antenna is assumed located on the ground with relative height difference of zero. This assumption allows the lower half of the terrestrial station radiation pattern to be cut off, thus making no contribution to interference. The cumulative distribution of transmission loss, L and effective transmission loss, Le are computed with the 3D model of Awaka simplified coupling prediction program. The frequency range of interest is 4 – 35 GHz. Both vertical and horizontal polarizations are considered in this study for convective rain cell. Thunderstorm rain characteristics of the tropical paths are taken into account.

3.2.3 METEROLOGICAL PARAMETERS

The convective tropical rain is often generated in the cumulonimbus clouds; they are convective cells consisting of active centers with strong up and down drafts. They are also structured as hydrometeor with high falling intensity, accompanied with thunderstorm. In most part of the tropics, the mean freezing height (h_{FR}) under raining conditions varies from 4.54 -4.79km for all distributions considered in this study. (h_{FR}) is expected to remain constant throughout the region. The mean annual cumulative distribution of point rain rate P(R) measured in Akure were used in this study.

Figure 3.1 illustrates typical hydrometeor scatter geometry from a terrestrial system to an earth- space system. The path geometry of hydrometeor scatter interference is defined in terms of the station separation, their projection to the common volume and also their bearings. Table 3.1 Shows the basic input parameters needed for the modeling.

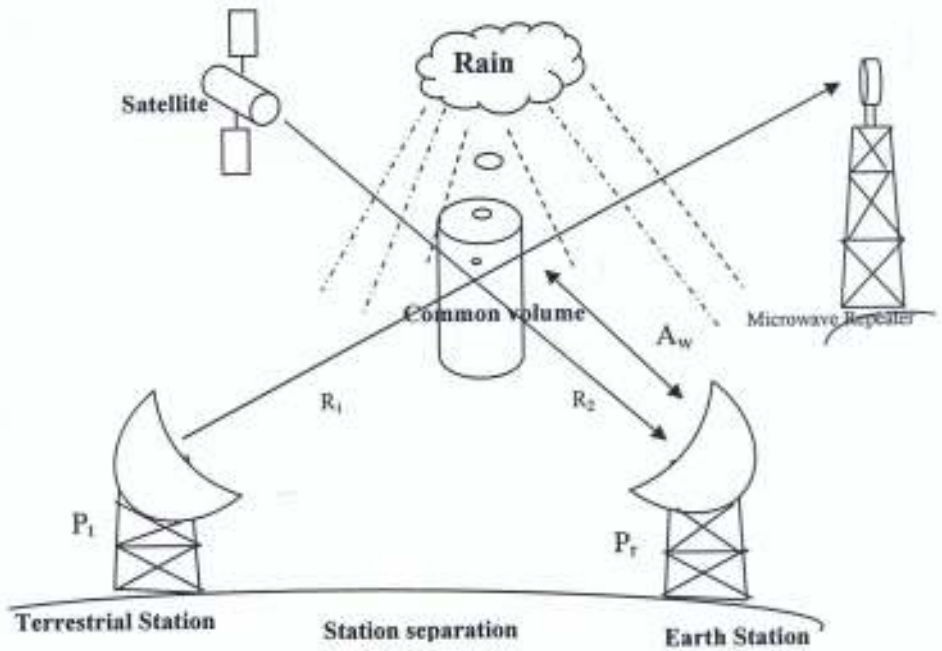

Fig 3.1: Hydrometeor scatter geometry between a terrestrial microwave station and a satellite downlink receiver operating at the same frequency, (as reported by Ojo et al.,2008).

Table 3.1: List of basic input parameters needed for evaluation of transmission loss

Link Parameters	
Station	Akure, Nigeria
Location	(Long $5^0\ 11^1$ E, Lat $7^0\ 15^1$N)
Frequency range	4 -35 GHz (Ku and Ka –bands frequencies)
Path length	50 – 250km
Electrical Characteristics of the link	
Satellite Earth Station	
Antenna	Gaussian radiation pattern
Gain	59dB
Beam Width	0.18^0
Efficiency	55%
Elevation Angles	55^0, 23^0 and 42.5^0
Interfering Terrestrial Station	
Elevation angle	1^0
Beamwidth	1.6^0
Antenna gain	35 – 55dB
Polarization	Vertical and Horizontal
Meteorological Parameters	
Rainfall type	thunderstorm rain type
h_{FR}	4.54 – 4.79 km
Mean annual rainfall	624mm/h
Average water vapour	$20g/m^3$
Water Temperature	20^0C
Z – R relation	$\frac{461\ R^{1.31}}{20}$

CHAPTER FOUR

RESULTS AND DISCUSSIONS

The modified Awaka 3 – dimensional rain cell model has been used to estimate the statistics of the transmission loss and the effective transmission loss for terrestrial station to common volume distance (TS- CV) ranging from 50.7 km for short path length and 204km for long path length. The result obtained are compared in the frequency range (6 - 35 GHz) for effective transmission loss, Le(dB) and transmission loss, L(dB) at 0.01% and 0.001% time of unavailability (outage time).

4.1 Variations of Transmission Loss, L with Percentage (%) of Time

Figure 4.1 shows the variation of transmission loss, L(dB) with the percentages of time at 45dB gain over elevation angles of 55°, 23° and 42.5°, frequency of 16 GHz and for short path length of 50.7km for both horizontally and vertically Polarized signals.

For the vertical polarization, the transmission loss varies from between 120.3 and 127.3 dB; 116.1 and 120.1 dB; and 118.4 and 127.4 dB for look angles of 55°, 23°, 42.5° respectively.

The result obtained for the horizontal polarization has a slight difference with the result of the vertical polarization. The transmission loss varies from about 121.3 to 128.3 dB; 117.1 to 127.1 dB; and 119.4 to 128.4 dB for the look angles of 55°, 23° and 42.5° respectively. Hence at 16 GHz there exists a higher transmission loss statistics computed for the elevation angle of 42.5° as compared with the other look angles in this study. This predicts a lesser interference for the percentages of occurrence ranging from 10^{-1} to 10^{-3} for the elevation angle of NIGCOMSAT -1.

The comparison presented in Figure 4.2 for long path length at 16 GHz and station separation of 204 km shows that transmission loss values are higher when compared with the results over short path length at all the elevation angles considered. This may be due to the rapidly decreasing radar reflectivity in the ice region at long path length.

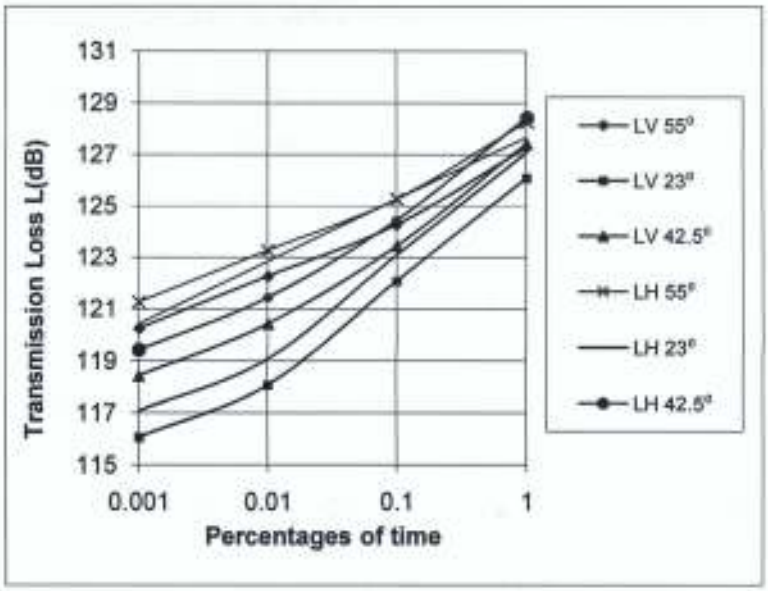

Fig 4.1: Variation of transmission loss with percentages of time at 16 GHz for short path length.

LV – transmission loss due to vertical polarization.
LH – transmission loss due to horizontal polarization.

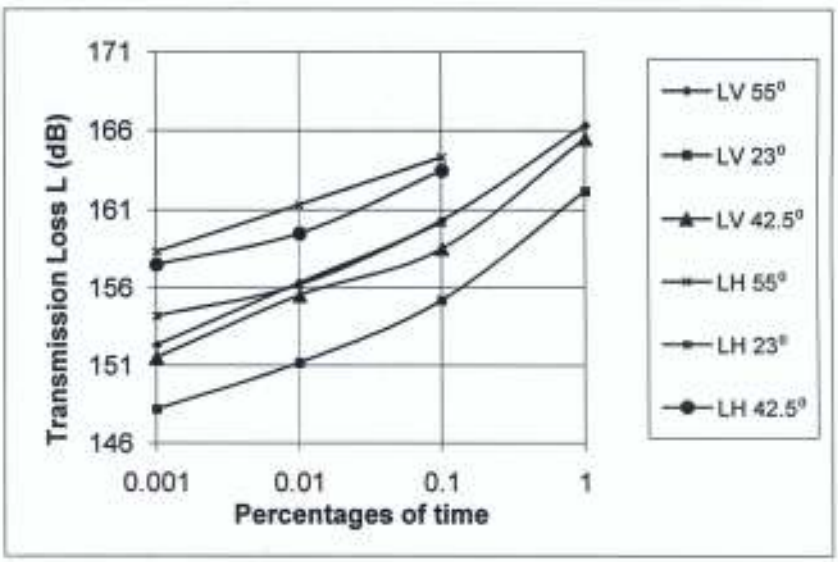

Fig. 4.2: Variation of transmission loss with percentages of time at 16 GHz for long path length.

LV – transmission loss due to vertical polarization.
LH – transmission loss due to horizontal polarization .

4.2 Variation of Transmission loss, L with station separation TS –CV (km)

The effect of varying terrestrial station to common volume distance on the computed transmission loss is examined over time percentages of 10^{-2} to 10^{-3} at 16 GHz for both vertical and horizontal polarizations. The comparison is shown in figures 4.3 and 4.4 over elevation angles of 55°, 23° and 42.5°. The result shows that the cumulative distribution of transmission loss increases gradually with increasing station separation, irrespective of the elevation angles. This implies less interference in the satellite receiving system. This same trend was also observed at 16 GHz frequency for 0.001% of time as presented in figure 4.4, for example, the transmission loss for satellite look angle 55° ranges from about 122.3 to 156.3 dB; while for 23° elevation angles it ranges from 118.1 to151.2 dB; and at 42.5° it ranges from 120.4 to 155.5 dB at 0.01% of time for 16 GHz. However, at 0.001% of time, lower values of cumulative transmission loss were obtained which signifies higher interference in the satellite receiving systems. The result obtained for horizontal polarization shows a similar trend with an increment of about 1 dB for all the look angles.

Figure 4.5 presents the results of the variation of the transmission loss with station separation at the higher frequency of 20 GHz for 0.01%. The result obtained from the cummulative distribution of transmission loss at this frequency also shows a gradual increase with increasing TS-CV distance station separation greater than 100 km. However, the transmission loss is higher for 20 GHz thus implying lesser interference for 20 GHz than that of 16 GHz.

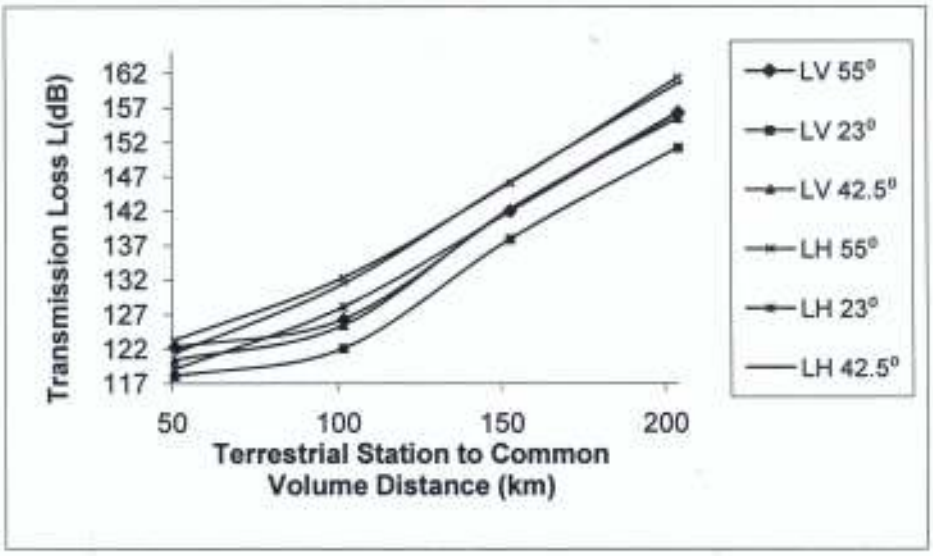

Fig.4.3: Variation of transmission loss with terrestrial station to common volume distance (TS – CV) at 0.01% of time for 16 GHz Scattering.

LV – transmission loss due to vertical polarization.
LH – transmission loss due to horizontal polarization.

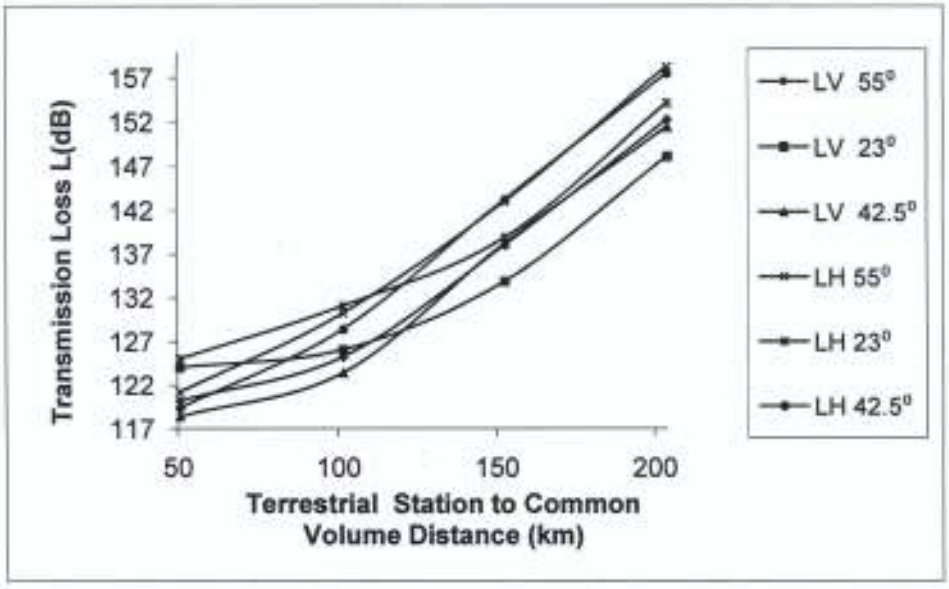

Fig. 4.4: Variation of transmission loss with terrestrial station to common volume distance (TS – CV) at 0.001% of time for 16 GHz scattering.

LV – transmission loss due to vertical polarization.
LH – transmission loss due to horizontal polarization.

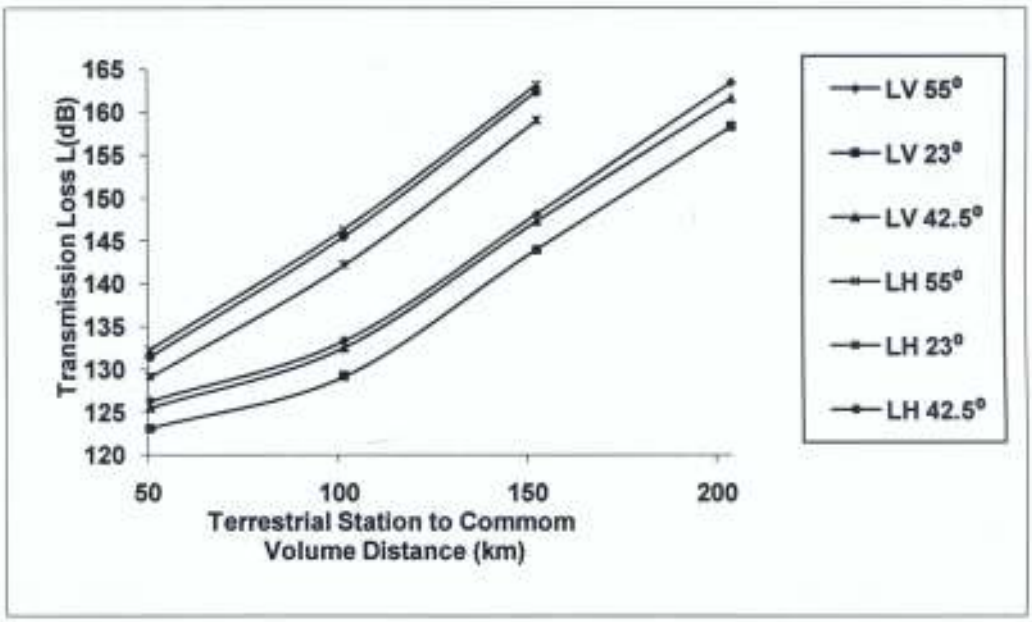

Fig 4.5: Variation of Transmission Loss with terrestrial station to common volume distance (TS – CV) at 0.01% of time for 20 GHz scattering.

LV – transmission loss due to vertical polarization.
LH – transmission loss due to horizontal polarization.

4.3 Variation of Transmission loss, L with Frequency

The effect of varying frequency on the computed transmission loss is also examined over varying terrestrial propagation path lengths at time percentages of 0.01% for both short and long path lengths. This is computed for frequency range of 6 to 35 GHZ, for both vertically and horizontally polarized signals. The variation is shown in figures 4.6 and 4.7 over short and long path length. The statistics of the transmission loss computed at the specific gain of 45 dB for short path length and for vertically polarized signals vary from about 117.8 to 127.5 dB; 115.6 to 125.3 dB; 116.9 to 120.4 dB for elevation angles of 55°,23° and 42.5° respectively. The results obtained for horizontal polarization range from about 117.8 dB to 138.6 dB for 55°; 115.6 dB to 131.3 dB for 23° and 116.9 dB to 132.7dB for 42.5°. It could be observed that at the higher frequencies of 20 GHz and 35 GHz, the transmission loss is significantly higher than at other frequencies for this path length due to the strong path length attenuation. For the long path length shown in figure 4.7, the values of L range between 161.8 dB, and 163.4 dB, for 55°; 156.0 dB and 158.3 dB for 23° and 160.0 dB and 161.6 dB for 42.5° at the specified frequencies. This result shows that at the frequencies investigated, transmission losses are higher for all look angles considered. This also predicts lesser interference compared with the short path length variations. The same trend could be observed at 0.001% of time (Fig 4.8). The results obtained when compared at both short path length and long path length are lower in all respects to values obtained for the 0.01% of time. This implies that at these frequencies, higher interference will occur at the 0.01% of time than at 0.001% of time for short path length.

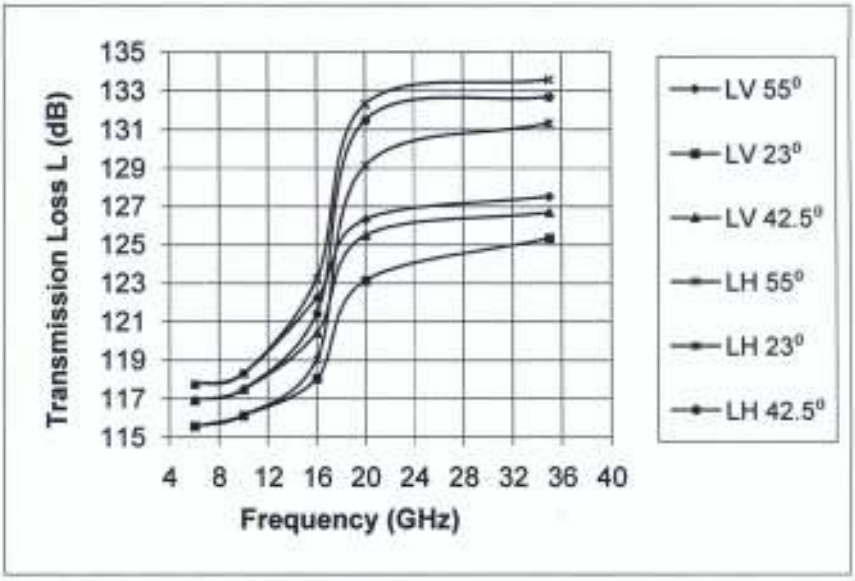

Fig 4.6: Variation of transmission loss with frequency in GHz for short path length at 0.01% of time.

LV – transmission loss due to vertical polarization.
LH – transmission loss due to horizontal polarization.

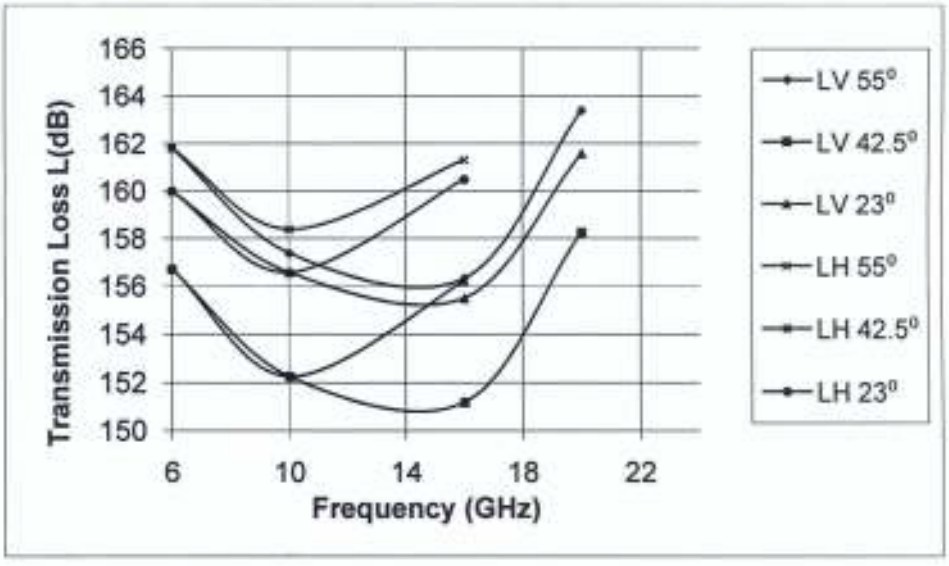

Fig 4.7: Variation of transmission loss L (dB) with frequency in GHz for long path length at 0.01% of time.

LV – transmission loss due to vertical polarization.
LH – transmission loss due to horizontal polarization.

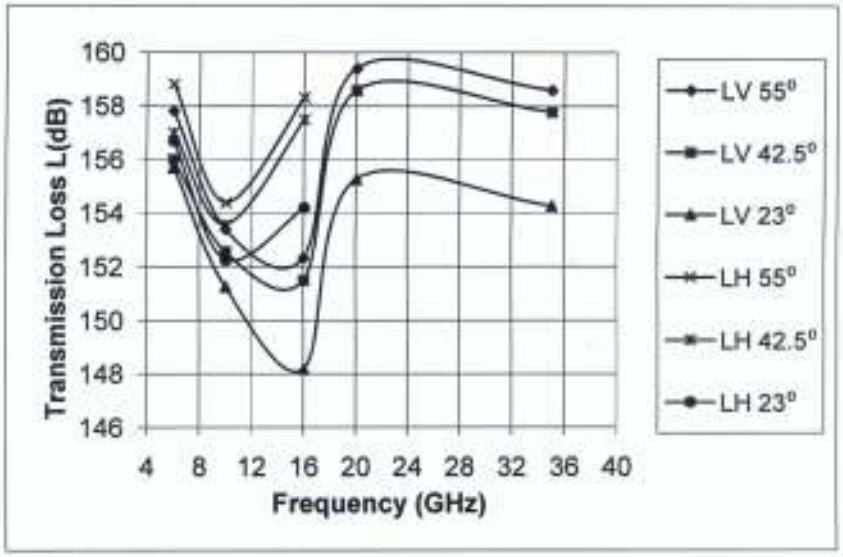

Fig 4.8: Variation of transmission loss with frequency in GHz for long path length at 0.001% of time.

LV – transmission loss due to vertical polarization.
LH – transmission loss due to horizontal polarization.

4.4 Variation of Transmission Loss, L with antenna Gain

The variation of the transmission loss is also made with the terrestrial antenna gain at 35 -55 dB for incidence wave signal at the look angles of 55°, 23° and 42.5°. The variation is made for the frequency of 16 GHz for short path length and long path length. Figures 4.9 and 4.10 show the variations at the frequency of 16 GHz for short path length and long path length and for 0.01% of time. The results from figure 4.9 show that for a given terrestrial gain, the cumulative distribution of transmission loss increases with increasing probability. This shows that transmission loss decreases linearly with increasing antenna gain for a given percentage time. This is observed for all the elevation angles 55°, 23°, 42.5°. For example for elevation of 55°, transmission loss decreases from about 132.3 dB to 112.3 dB; for 23°, 128.1 dB to 108.1 dB and 42.5°, 130.4dB to 110.4 dB for vertical polarization. This predicts a higher interference at 16 GHz for a short path length than for a long path length (204 km) as shown in figure 4.10, the cumulative transmission loss compared with the antenna gain gives higher values of transmission loss for 16 GHz frequency compared with the short path length.

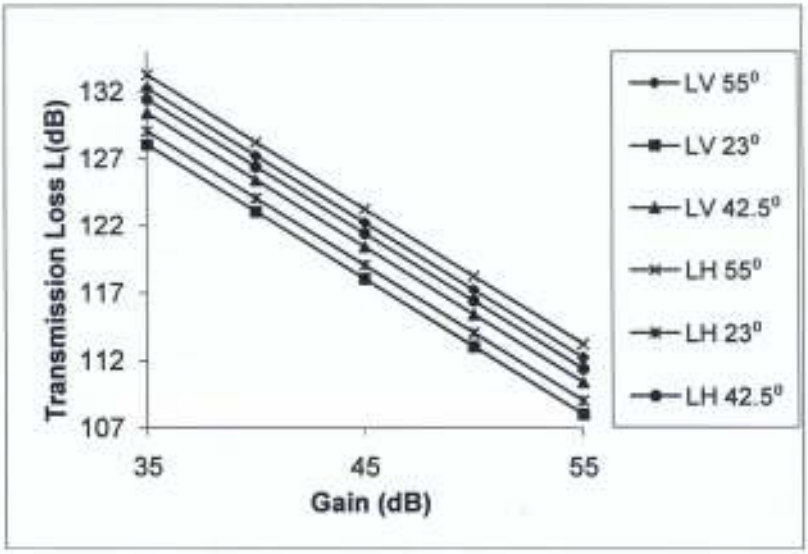

Fig 4.9: Variation of transmission loss with gain at 16 GHz for 0.01% of time for short path length.

LV – transmission loss due to vertical polarization.
LH – transmission loss due to horizontal polarization.

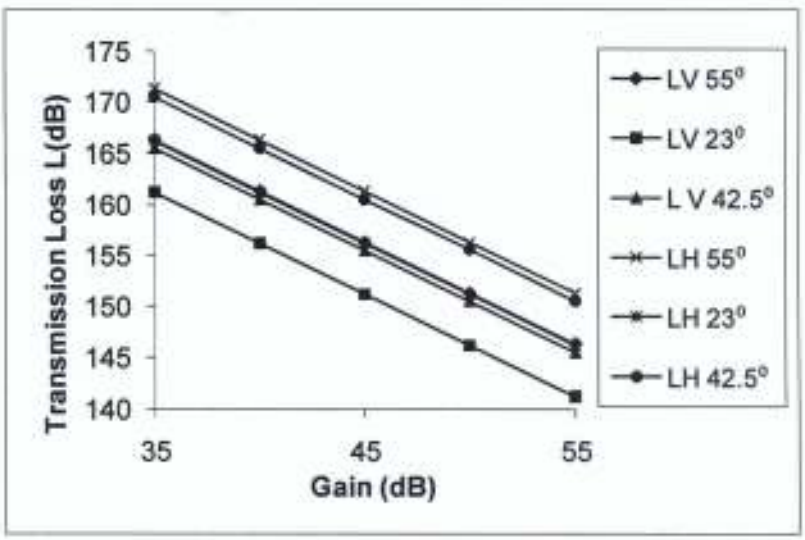

Fig 4.10: Variation of transmission loss with gain at 16 GHz for 0.01% of time for long path length.

LV – transmission loss due to vertical polarization.
LH – transmission loss due to horizontal polarization.

4.5 Evaluation of effective transmission loss, Le

The computed effective transmission loss, Le is as a result of the extra- attenuation due to rain on the wanted satellite signals for all the look angles employed in this study. In considering interference by rain scatter, statistics of the cumulative distribution of transmission loss alone is not sufficient to assess the severity of interference at the interfered stations. At higher frequencies, that is above 10 GHz, the wanted signal also suffers from attenuation due to hydrometeor scatter, signal degradation due to depolarization effect and scattering interference by precipitation particles (raindrop) along the radio paths. In locations with intense rain activity, the attenuation along the wanted path could be larger than the maximum link margin so that the satellite link would be out of service whatever the level of interference (Capsoni and D'Amico,1997).

4.5.1 Variation of effective transmission Loss with Percentage of time Unavailability.

Figure 4.11 presents the variation of the effective transmission loss with the percentage of time at antenna gain of 45 dB over the three elevation angles for short path length of 50.7 km.

The result shows clearly a lower cumulative effective transmission loss for all the look angles as compared with the statistics of cumulative transmission loss at the same frequency as presented in figure 4.1. This is due to the effect of the extra-attenuation. The values computed for the 16 GHz vertical polarization of the variation of effective transmission loss with percentages of time range from about 127.3dB to 116.3 dB for 55°; 124.1 dB to 113.1 dB for 23°; and 126.4 dB to 115.4 dB for 42.5° for vertically polarized signal for short path length. It also varies from 130.3 dB to 118.3 dB for 55°; 127.1 dB to 115.1 dB for 23° and 129.4 dB to 117.4 dB for 42.5° for horizontally polarized signal. However, the effect of the extra attenuation due to rain in the effective transmission loss relation is quite significant.

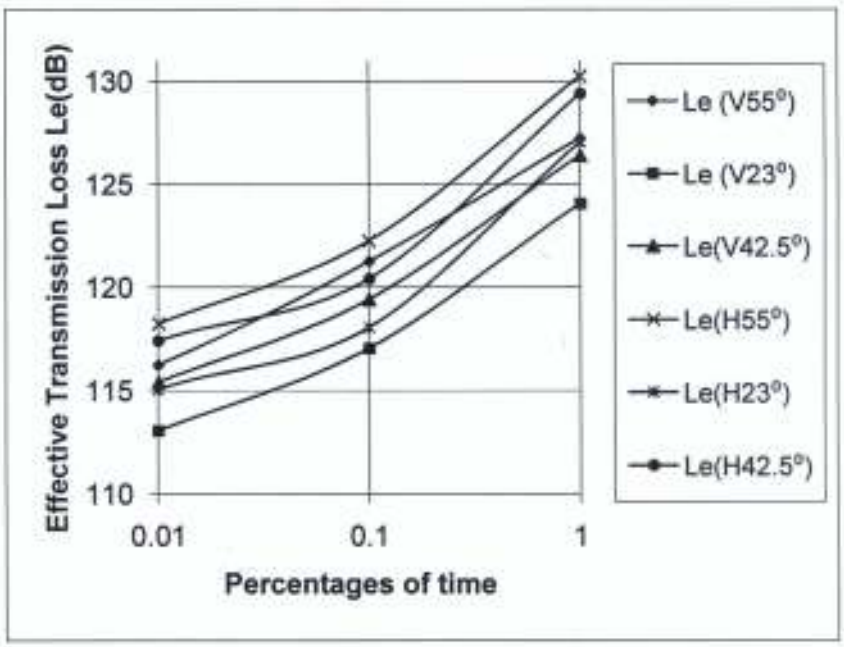

Fig 4.11: Variation of effective transmission loss with percentages of time at 16 GHz for short path length.

Le (V) – effective transmission loss due to vertical polarization.
Le (H) – effective transmission loss due to horizontal polarization.

4.5.2 Variation of Effective Transmission Loss, Le with Station Separation (TS-CV)

The comparison of effective transmission loss, Le (dB) with the terrestrial station to common volume distance is presented in Figure 4.12. The result was computed at various percentages of time ranging from $10^{-2} - 10^{-3}$ % at 16 GHz for polarizations considered in this study .The variation observed at 45 dB gain described that at this frequency, and for all the elevation angles considered the cumulative distribution of effective transmission Loss increases gradually with increasing station separation. However, the value is lower as compared to the transmission loss, this is due to the effect of the extra –attenuation along the wanted path.

Figure 4.13 shows the variation of the statistics of effective transmission loss with station separation at 20 GHz for the look angles of 55°, 23°, and 42.5°. The result shows a difference of about 2 dB over the different elevation angles.

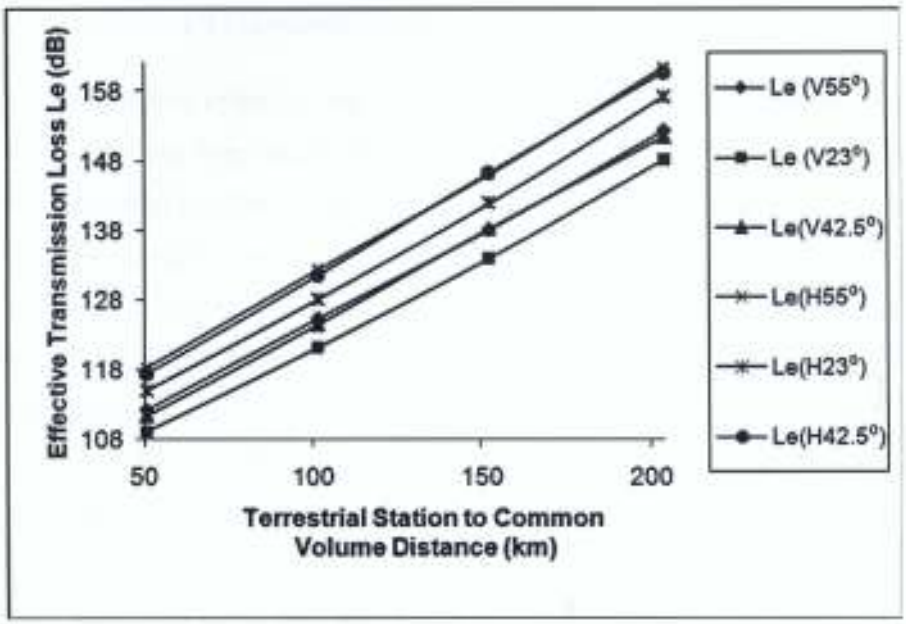

Fig. 4.12: Variation of effective transmission loss with terrestrial station to common volume distance (TS – CV) at 0.01% of time for 16 GHz scattering.

Le (V) – effective transmission loss due to vertical polarization.
Le (H) – effective transmission loss due to horizontal polarization.

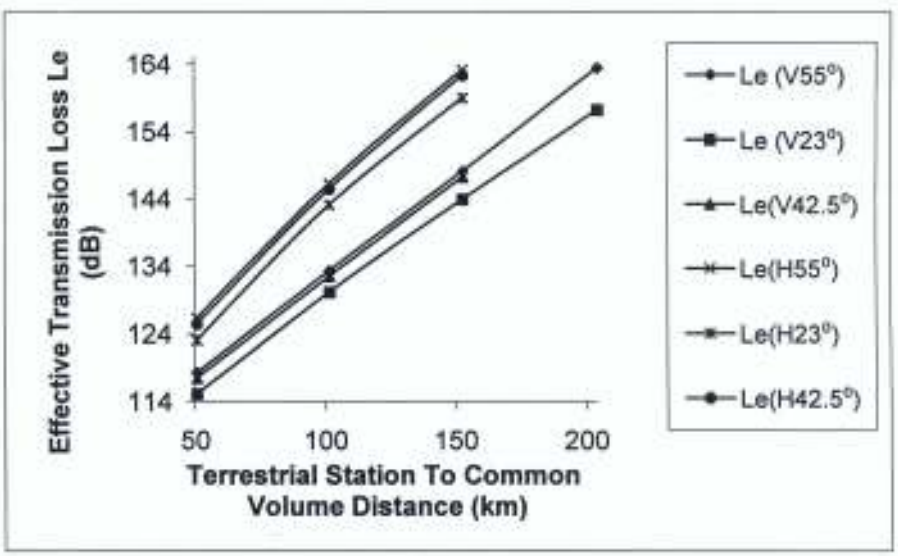

Fig. 4.13: Variation of effective transmission loss with terrestrial station to common volume distance (TS – CV) at 0.01% of time for 20 GHz scattering.

Le (V) – effective transmission loss due to vertical polarization.
Le (H) – effective transmission loss due to horizontal polarization.

4.5.3 Variation of Effective Transmission Loss, Le with Frequency

The results of some possible effects of the extra- attenuation on the wanted satellite signal are also considered for the frequencies of 6, 10, 16, 20 and 35 GHz. Figures 4.14 to figure 4.17 show the results of the variation of effective transmission loss compared with the frequencies at the elevation angles considered.

In figure 4.14, the result shows that at all the elevation angles the effective transmission loss, Le decreases with frequency in the frequency window between (6 - 16 GHz). However, in the frequency window (20 - 35 GHz), effective transmission loss decreases with a gentle slope. For the elevation angle of 55°, the effective transmission loss is about 122.8 dB to 116.3 dB, there is a decrease of Le with increasing frequency except in the frequency window of (16 - 20 GHz) where there is an exponential increase. For elevation angle of 23^0, Le varies between 119.6 dB to 113.1 dB in the frequency range (6 -16 GHz), while for the elevation angle of 42.5^0, Le varies between 121.9 dB to 115.4 dB.

Figure 4.15 shows the variation of effective transmission loss at different frequencies for 0.01% of time and at long path length of 204 km. The effect of the radar reflectivity factor Z is conspicuous at this larger path length as compared to the short path length. The common volume at this distance is in the ice region, hence ice scattering predominate over rain scattering. However, at long path length, effective transmission loss Le decreases up to 10 GHz, but started increasing at the frequency of 16 GHz. This is due to the decrease in the radar reflectivity factor in the in the ice region and the strong path length attenuation.

Figure 4.16 and Figure 4.17 shows the variation at 0.001% of time. It could also be observed that Le decreases with frequency except in the frequency window (6 -16 GHz) where there is predominance of interference.

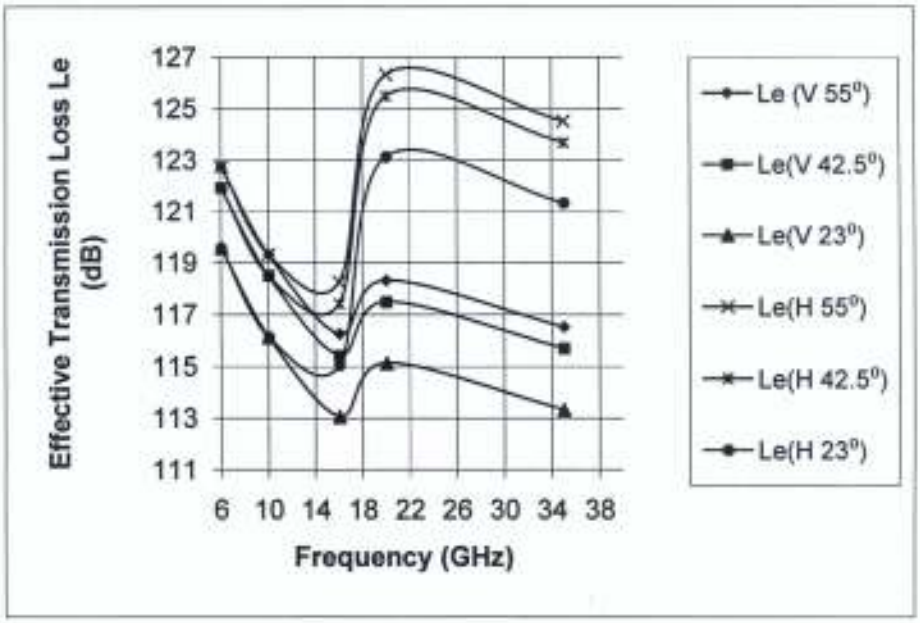

Fig 4.14: Variation of effective transmission loss with frequency in GHz for short path length at 0.01% of time.

Le (V) – effective transmission loss due to vertical polarization.

Le (H) – effective transmission loss due to horizontal polarization.

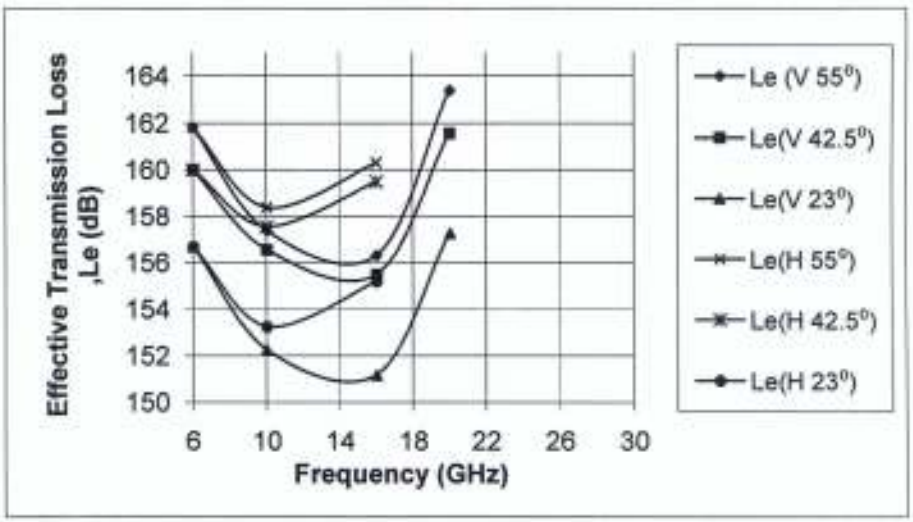

Fig 4.15: Variation of effective transmission loss with Frequency in GHz for long path length at 0.01% of time.

Le (V) – effective transmission loss due to vertical polarization .

Le (H) – effective transmission loss due to horizontal polarization.

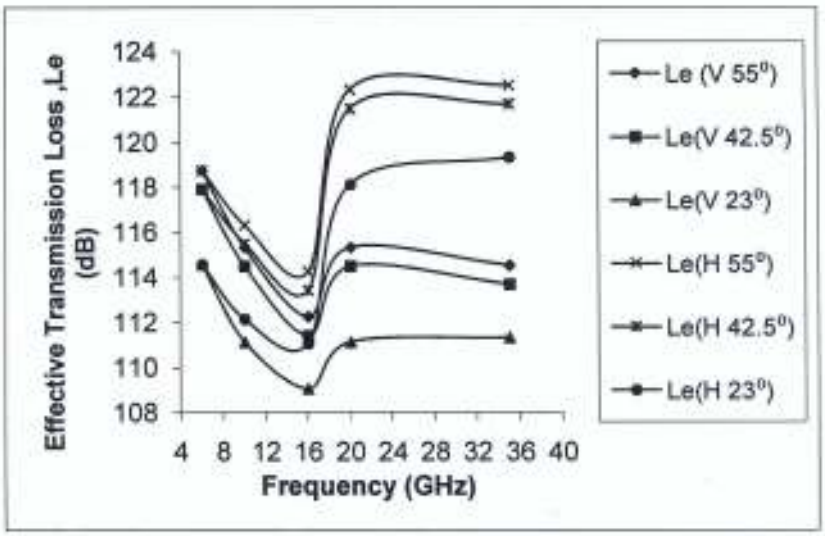

Fig 4.16: Variation of effective transmission loss with frequency in GHz for short path length at 0.001% of time.

Le (V) – effective transmission loss due to vertical polarization.
Le(H) – effective transmission loss due to horizontal polarization.

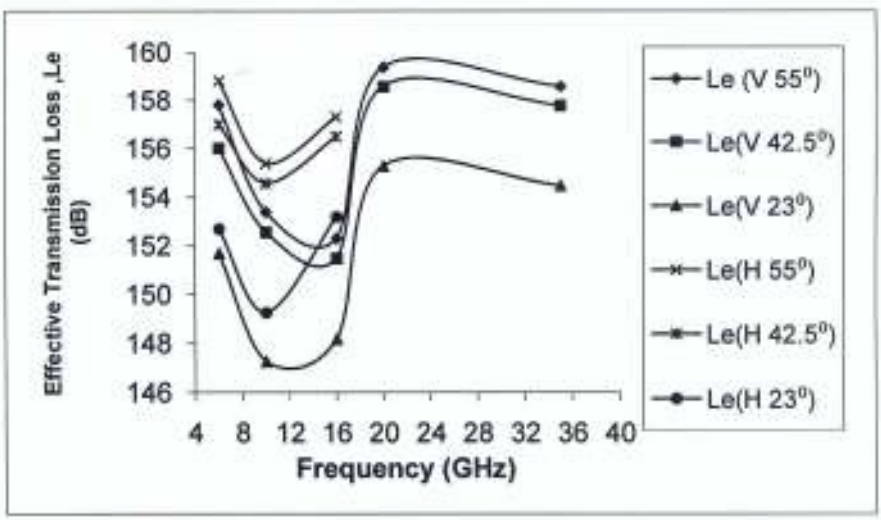

Fig 4.17: Variation of Effective Transmission Loss L(dB) Against Frequency in GHz for Long Path Length at 0.001% of time.

Le (V) – effective transmission loss due to vertical polarization.
Le (H) – effective transmission loss due to horizontal polarization.

4.5.4 Variation of Effective Transmission Loss with Antenna Gain

Figure 4.18 presents a typical variation of effective transmission loss, Le with antenna gain for both vertical and horizontal polarizations at the frequency of 16 GHz. The result shows that the horizontally polarized signal gives in most cases lower statistics of effective transmission loss, Le compared with the vertically polarized signal.

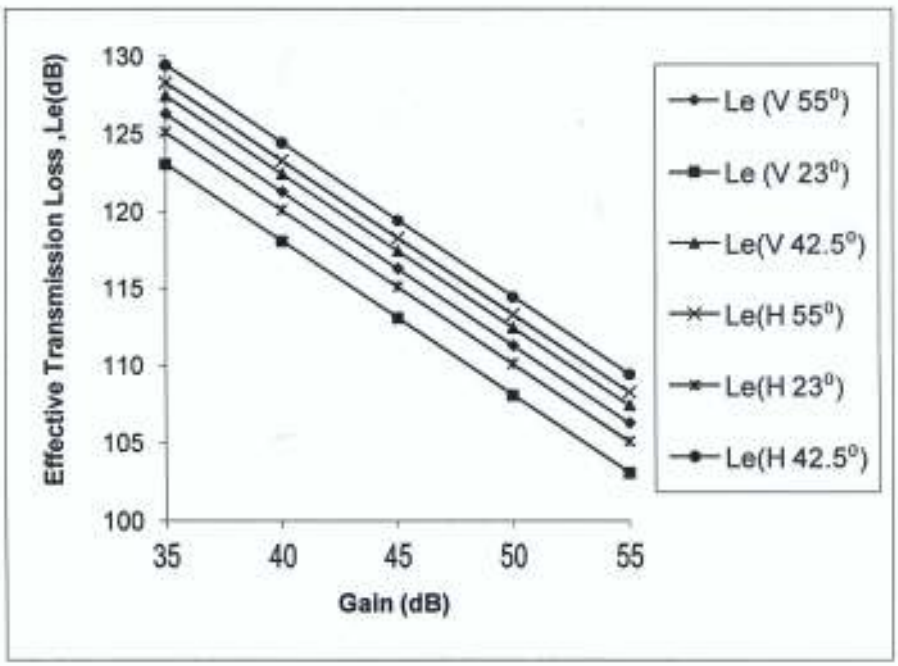

Fig 4.18: Variation of effective transmission loss with antenna gain for 0.01% of time for short path length.

Le (V) – effective transmission loss due to vertical polarization.
Le (H) – effective transmission loss due to horizontal polarization.

4.6 Comparisons of effective transmission loss, Le (dB) and transmission loss, L (dB) with percentages of time.

The results of the comparison of effective transmission Loss and the transmission loss with percentages of occurrence ranging from 10^{-3} to 1% were also presented in figures 4.19 - 4.21 for the two polarizations considered. The result shows that both L and Le increases as the percentage of time increases irrespective of the elevation angle, although, the result at the look angle of 55° is higher than other elevation angles. This shows that signal through elevation angle of 55° suffer lesser interference as compared to the other elevation angles considered in this study. The effect of the extra attenuation was observed for the effective transmission loss. The result for the frequency of 16 GHz agrees with the statement that at frequencies higher than 10 GHz the wanted signal suffers much attenuation due to hydrometeor scatter, in addition to signal degradation due to depolarization effects.

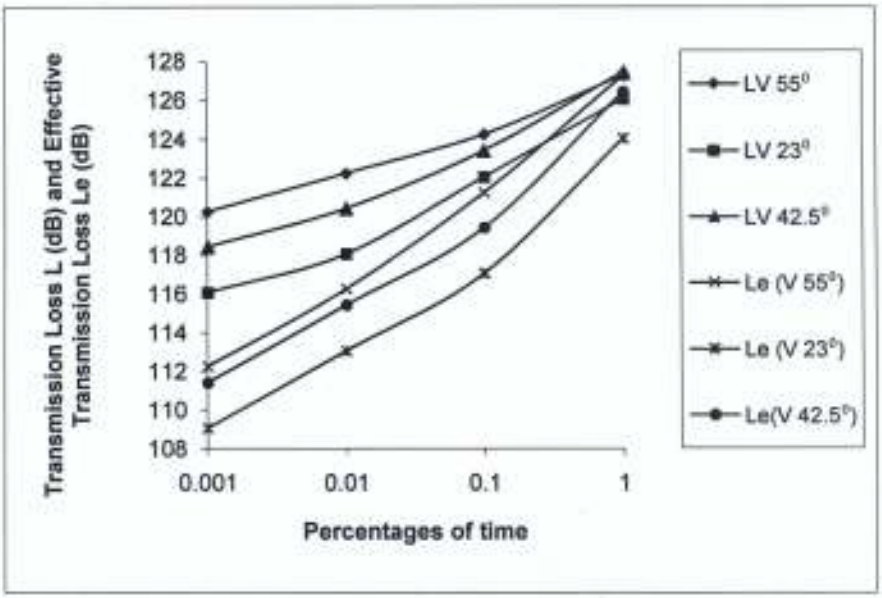

Fig 4.19: Comparison of transmission loss and effective transmission loss with percentages of time at 16 GHz Scattering for vertically polarized signals.

L (V) – transmission loss due to vertical polarization.
Le(V) – effective transmission loss due to vertical polarization.

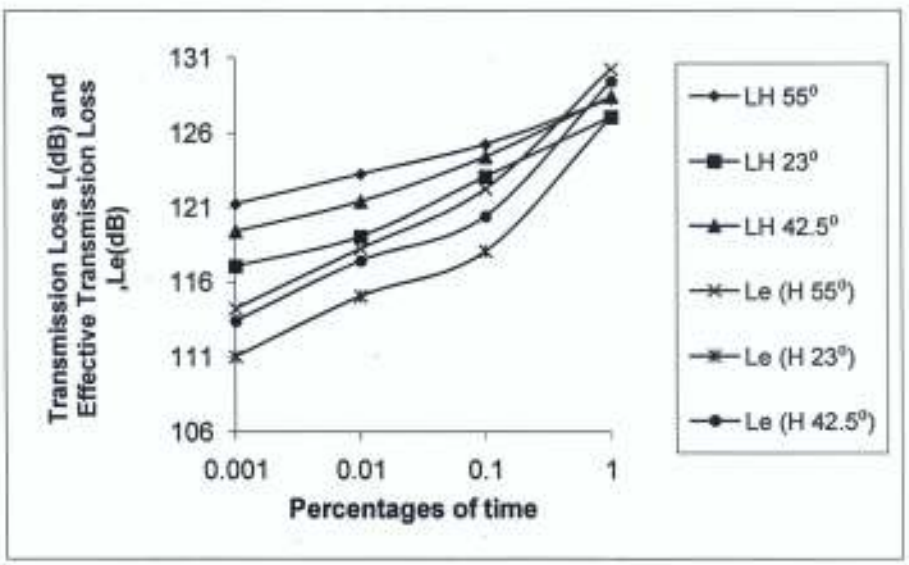

Fig 4.20: Comparison of transmission loss and effective transmission loss with percentages of time at 16 GHz scattering for horizontally polarized signals.

L (H) – transmission loss due to horizontal polarization.
Le (H) – effective transmission loss due to horizontal polarization.

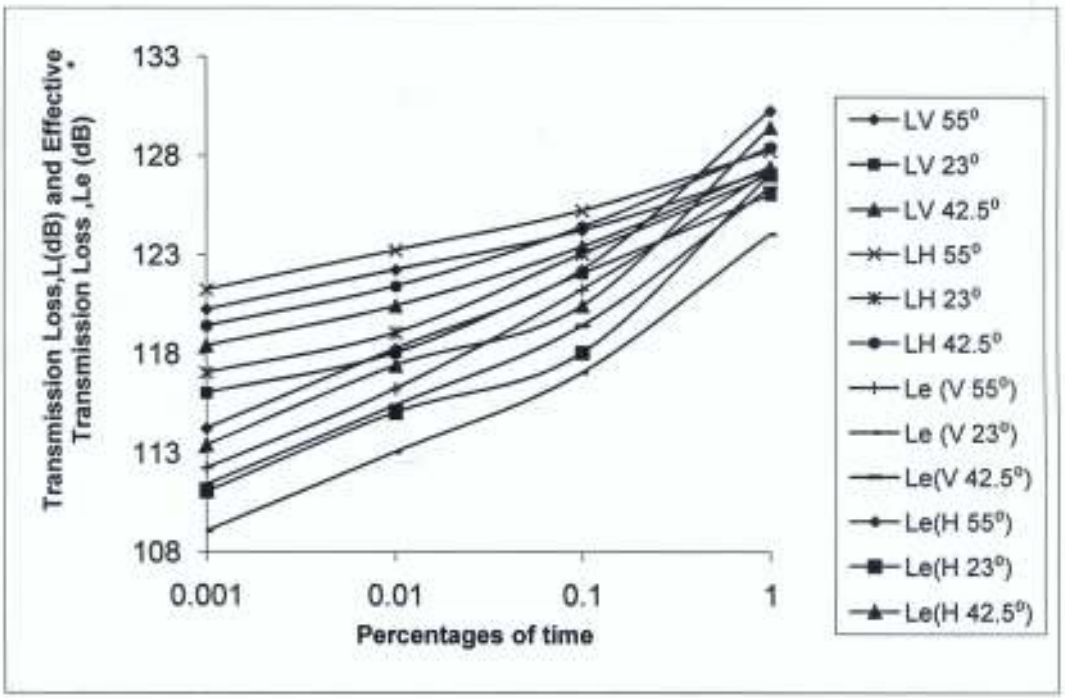

Fig 4.21: Comparison of transmission loss and effective transmission loss with percentages of time at 16 GHz scattering for vertically and horizontally polarized signals.

L (V) – transmission loss due to vertical polarization.
Le(V) – effective transmission loss due to Vertical polarization.
L (H) – transmission loss due to horizontal polarization.
Le(H) – effective transmission loss due to horizontal polarization.

4.7 Comparisons of effective transmission loss, Le(dB) and transmission loss, L(dB) with station separation.

Figures 4.22 to 4.25 compare the effective transmission loss and transmission loss with the terrestrial station to common volume distance (TS-CV). The comparisons show that antenna gain increase with increasing probability. This is observed at percentage of time of 0.01% of time. For example in Figure 4.22, the observed effective transmission loss varies from about 112.3 dB to 152.3 dB; 109.1dB to 148.2 dB and 111.4 dB to 151.5 dB for elevation angles of 55°, 23°, 42.5° respectively for vertically polarized signals. For horizontally polarized signals, it varies from about 118.3 dB to 161.3 dB; 115.1dB to157.2 dB and 117.4 dB to 160.5 dB for the look angles 55°, 23° and 42.5° respectively. For the transmission loss L(dB) and short path length the values vary from about 120.3 dB to 152.3 dB; 124.1 dB to 148.2 dB and 118.4 dB to151.5 dB for 55°, 23°, 42.5° respectively for vertically polarized signals. Also 121.3 dB to158.3 ; 125.1 dB to 154.2 dB and 119.4 dB to 157.5 dB at the look angles 55°,23°,and 42.5° respectively for the horizontally polarized signals. The result predicts that transmission loss is higher when compared with the computed values of the effective transmission loss. This is as a result of the extra attenuation on the effective transmission loss.

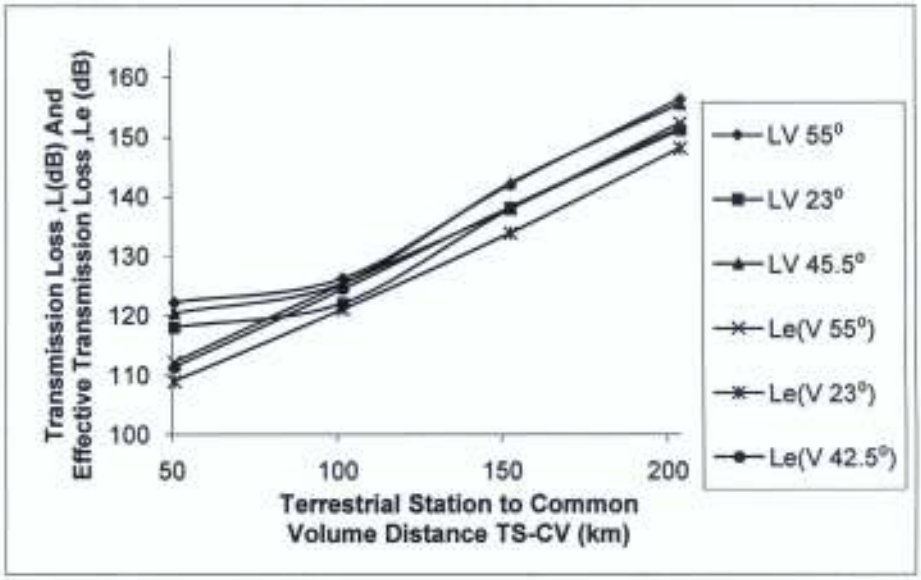

Fig 4.22: Comparison of transmission loss and effective transmission loss with (TS-CV) at 0.01% of time for 16GHz scattering for vertically polarized signals.

L (V) – transmission loss due to vertical polarization.

Le (V) – effective transmission loss due to vertical polarization.

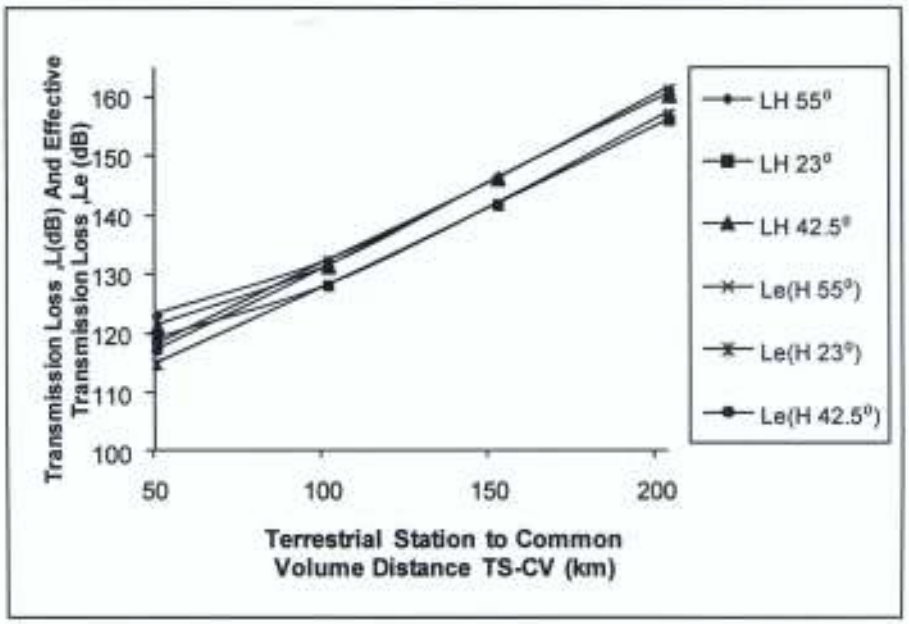

Fig 4.23: Comparison of transmission loss and effective transmission loss with (TS-CV) at 0.01% of time for 16GHz scattering for horizontally polarized signals.

L (H) – transmission loss due to horizontal polarization.

Le (H) – effective transmission loss due to horizontal polarization.

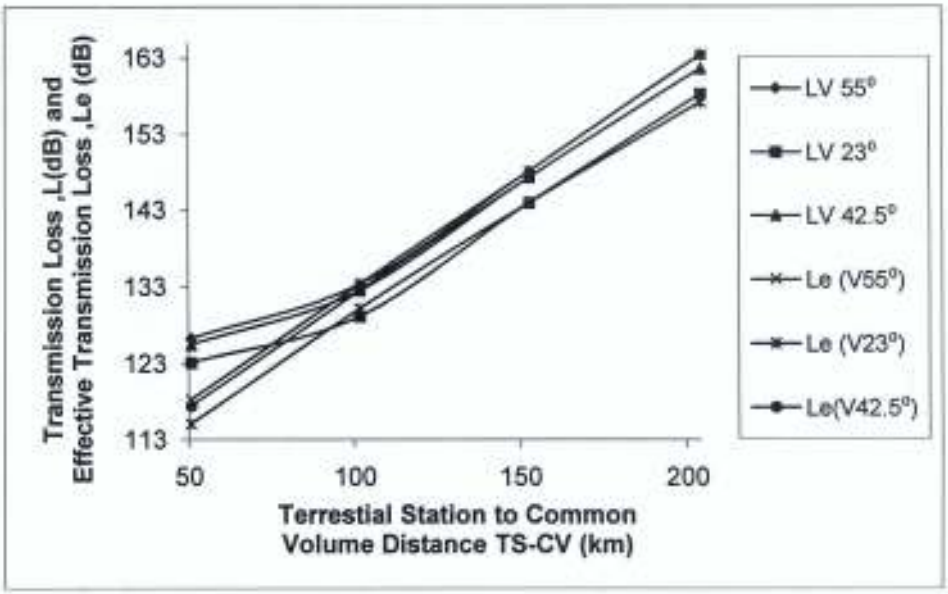

Fig 4.24: Comparison of transmission loss and effective transmission loss with TS-CV at 0.01% of time for 20GHz scattering for vertically polarized signals.

L (V) – transmission loss due to vertical polarization
Le(V) – effective transmission loss due to Vertical polarization.

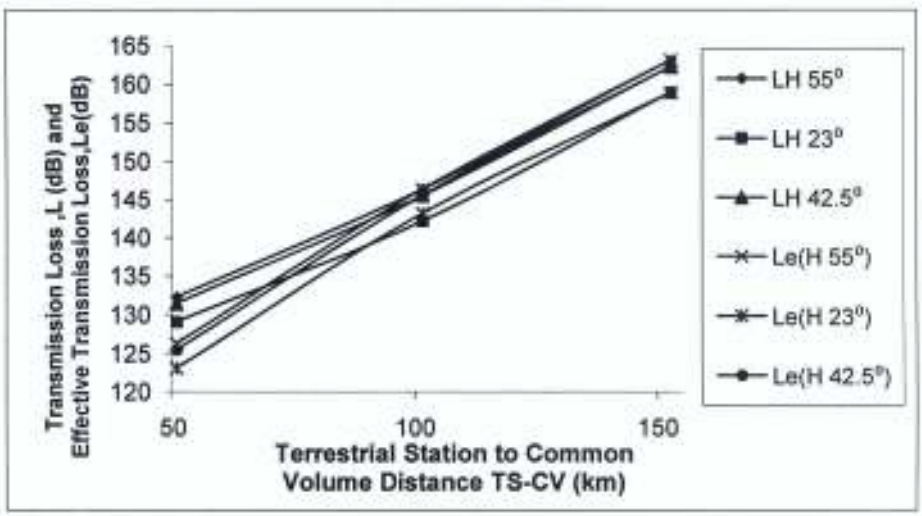

Fig 4.25: Comparison of transmission loss and effective transmission loss with TS-CV at 0.01% of time for 20 GHz scattering for horizontally polarized signals.

L (H) – transmission loss due to horizontal polarization.
Le (H) – effective transmission loss due to horizontal polarization.

4.8 Comparison of transmission loss, L (dB) and effective transmission loss, Le (dB) with frequency.

Figure 4.26 shows the variation of transmission loss and effective transmission loss with frequency. The results show a difference of about 5dB between L and Le.

In figures 4.27 and 4.28 at percentage of time of 0.01 %, it was observed that at the frequency range of (6 – 35 GHz) there is predominance of lower transmission loss around 10 GHz for effective transmission loss and transmission loss for both polarizations.

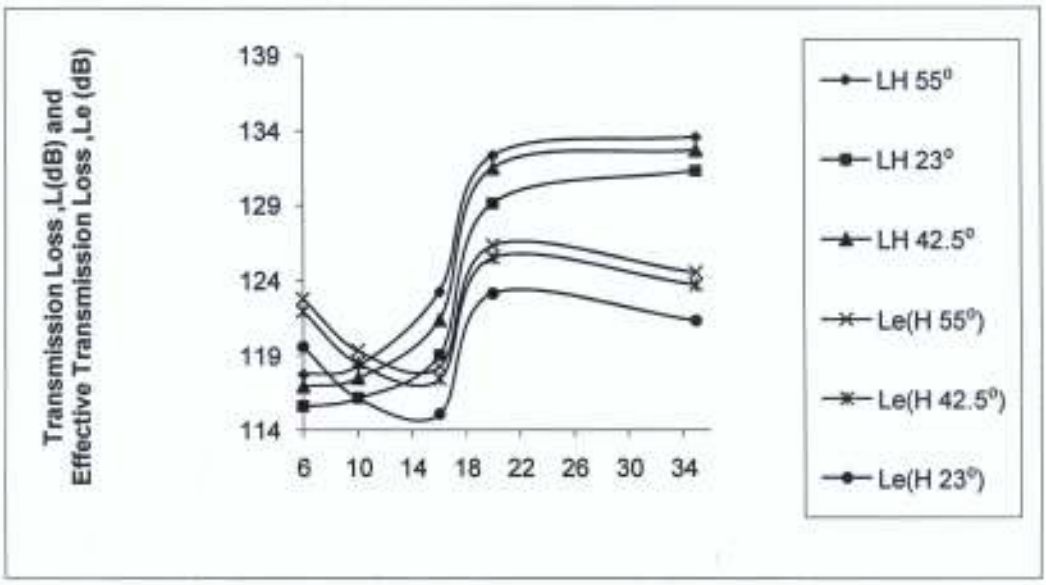

Fig 4.26 Comparison of transmission loss and effective transmission loss with frequency in GHz at 0.01% of time for short path length of horizontally polarized signals.

L (H) – transmission loss due to horizontal polarization.
Le (H) – effective transmission loss due to horizontal polarization.

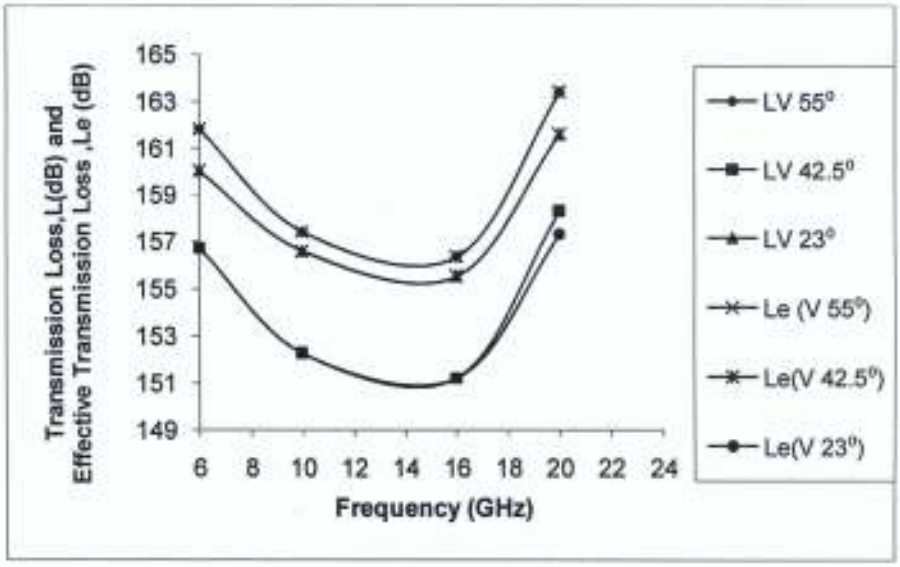

Fig 4.27: Comparison of transmission loss and effective transmission loss with frequency in GHz at 0.01% of time for long path length of vertically polarized signals.

L (V) – transmission loss due to vertical polarization.
Le (V) – effective transmission loss due to vertical polarization.

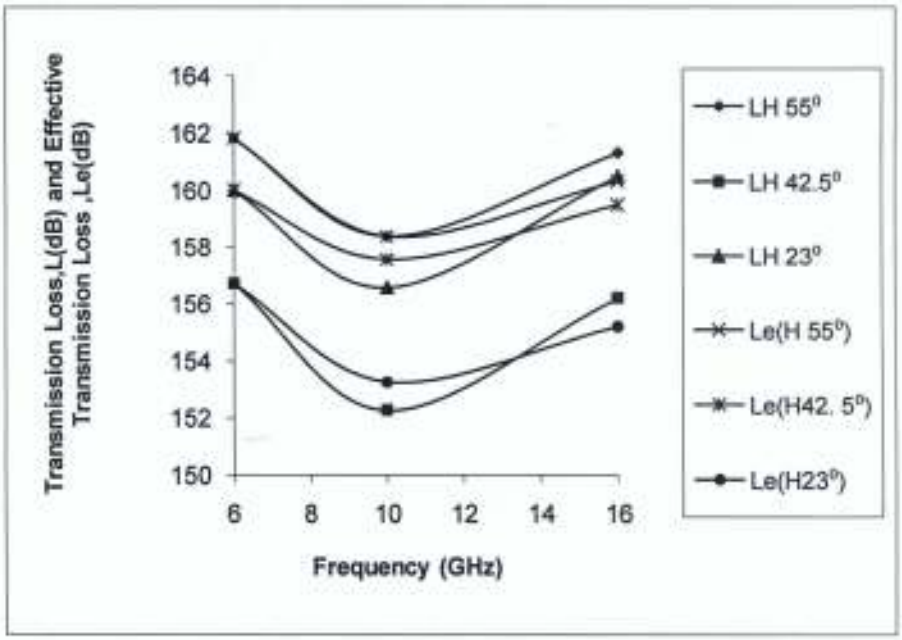

Fig 4.28: Comparison of transmission loss L and effective transmission loss with frequency in GHz at 0.01% of time for long path length of horizontally polarized signals.

L (H) – transmission loss due to horizontal polarization.
Le (H) – effective transmission loss due to horizontal polarization.

CHAPTER FIVE

5.0 CONCLUSIONS

In this dissertation, the cumulative distribution of the transmission loss L, and the effective transmission loss, Le are estimated using the modified version of 3D bistatic radar equation of the Awaka model. Practical radio propagation parameters such as antenna beamwidth, antenna gain and antenna separation distance from the satellite to the common volume formed by the intersecting signals and their effects on transmission loss have been investigated. The results obtained are compared over three elevation angles of 55° (over the Atlantic Ocean Region), 23° (Indian Ocean Region) and 42.5° (NIGCOMSAT-1 geostationary satellite) for both vertically and horizontally polarized radio signals .

The results presented show that at frequencies higher than about 10 GHz and antenna separation longer than about 170 km, the common volume formed by the intersecting beam will be in the ice region where attenuation decreases at the rate of 6.5 dB/km, irrespective of the look angles. Under this condition, transmission loss tends to decrease with increasing frequency portending higher interference level in the interfered station. This characteristic was observed for both vertically and horizontally polarized radio signals.

The effective transmission loss was observed with the significance of the extra attenuation, signal degradation due to depolarization effect and scattering interference by the precipitated particles (raindrop) along the radio paths. The result presented also shows that the transmission loss decreases linearly with increasing terrestrial antenna gain for a given probability level. Also, evaluation of the effective transmission loss shows that additional attenuation weakens the received signal. This was observed for all the look angles 55°, 23° and 42.5°.

However, the results of the transmission loss due to the rain scatter obtained in this study will provide good estimates to check the severity of rain scattering on communication channels particularly at Ku band (11/14 GHz) and Ka band (20/30 GHz) during thunderstorm rainfall activity. This is in particular noticeable during signal outage on direct to home (DTH) very small antenna terminal (VSAT) services.

5.1 RECOMMENDATIONS

It is recommended that investigation of some practical radio propagation parameters such as rain freezing height (h_{FR}), antenna beamwidth, radar reflectivity to rain rate relation and transmission loss to radar reflectivity relation (L to Z) algorithm be carried out as a matter of urgency. Using appropriate parameters for each location of study to evaluate transmission loss L, and the effective transmission loss, Le, may improve the results for the locations. However, it may not be easy to carry out such studies, as it requires some sophisticated instrumentation and substantial funding. Therefore, funding for research is therefore necessary to enhance better telecommunication services in the locations of interest.

REFERENCES

Ajayi, G.O and Owolabi, I.F (1987): Rainfall parameters from distrometer drop size Measurement at a tropical station, Ann. Telecomm, Vol. 42 No 1-2, p 4 - 12

Ajayi. G.O and Barbaliscia F. (1990): Prediction of attenuation due to rain characteristics of the 0 ^{0}C isotherm in temperate and tropical climates, Int. J. Satellite commun, Vol. 8, p 187 – 196.

Ajewole, M.O (2003): Bistatic Interference due to tropical rainfall types: a comparison of rain-cell model, Atti Della Fondazione Giorgion Ronchi, Vol58, 1 p 129-141.

Ajewole, M.O, Kolawole, L.B and Ajayi, G.O (1999): Evaluation of bistatic intersystem interference due to scattering by hydrometeor on tropical paths, Int. J. satellite comm. Vol. 17,p 339-356.

Ajewole, M.O and Ojo, J.S (2005): Intersystem interference due to hydrometeror scattering on satellite downlink signals in tropical location. African Journal of Science and Technology UNESCO (AJST), Kenya, 6(2), p 84 -93.

Awaka .J and Oguchi. T (1982) : Bistatic radar reflectivities of pruppacher – and –pitter form raindrop at 34.8 GHz , Radio sci. Vol.17, No1, p 269-278.

Awaka, J (1989). A Three dimensional rain cell models for the study of interference due to hydrometeor scattering. Journal of commu. Research Laboratory, Vol 36 No 147 p 13-44.

Capsoni, C, D'Amico, M, Martellucci, A, Oladano, L and Paraboni, A (1992): A 3D prediction method of scattering interference complete versus pencil beam approximation. Proc. URSI comm. F. Open. Symp. On wave propagation and remote sensing. Ravenscar England p 8-11.

Capsoni, C and D'Amico, M. (1997): A physically based, simple prediction method for scattering interference. Radio science, Vol. 32, No 2, p 397-407.

Capsoni, C, Fedi, F, and Paraboni, A. (1987a): A comprehensive meteorological orientated methodology for the prediction of wave propagation parameters in telecommunication application beyond 10GHz. Radio science, Vol 22. No3 p 387-393.

Capsoni, C, Fedi, F, Magistroni, C, Paraboni, A and Pawlina, A (1987b):Data and theory for a new model of the horizontal structure of rain cells for propagation applications, Radio Sci., 22(3), p395-404.

Commission of the European Communities on Cooperation in the fields of Scientific and Technical Research, COST 210: Influence of the atmosphere on interference between radio communication systems at frequencies above 1GHz, Final Rept, EUR 13407EN, Brussels, 1991.

COST 210, Report 569, 1990.

Crane, R. (1974): Bistatic scatter from rain, IEEE Trans. Ant. And Propag; A& P22, No2 p 312-320.

Holt, A.R, Mac Guinness, D.G, Chartton, Thompson P.T and Mehler M.J (1992): The development of a model to estimate the bistatic transmission loss associated with intersystem interference. IEEE Trans. Ant and Propag. Vol 41 No 10 p 1422-1430.

Marshall, J.S and Palmer, W.M.K (1948): The distribution of raindrops with size. J. Meteorol; Vol. 5, p 165-166.

Olsen, R. L. (1993); Interference due to hydrometeor scatter on satellite communication links. Proc. IEEE Vol.81 p 914-922.

Ojo, J.S, Sarkar S.K and Adediji, A.T (2008); Intersystem interference on horizontally polarized radio signal in tropical climate. Indian Journal of Radio and space Physics. Vol 37, p 408-413.

Ojo, J.S and Ajewole M.O (2010): Interference due to hydrometer scattering on horizontally polarized signal transmission through different types of tropical rainfall. Nigeria Journal of space Research (in press).